(4)

David Taylor Research Center

Bethesda, MD 20084-5000

DTRC SHD 1268-01 June 1988

Ship Hydromechanics Department

NEAR AND FAR FIELD PROPELLER WAKE STUDY USING LASER DOPPLER VELOCIMETRY

by

James N. Blanton

Scott Fish

DTRC SHD 1268-01 NEAR AND FAR FIELD PROPELLER WAKE STUDY
USING LASER DOPPLER VELOCIMETRY

MAJOR DTNSRDC TECHNICAL COMPONENTS

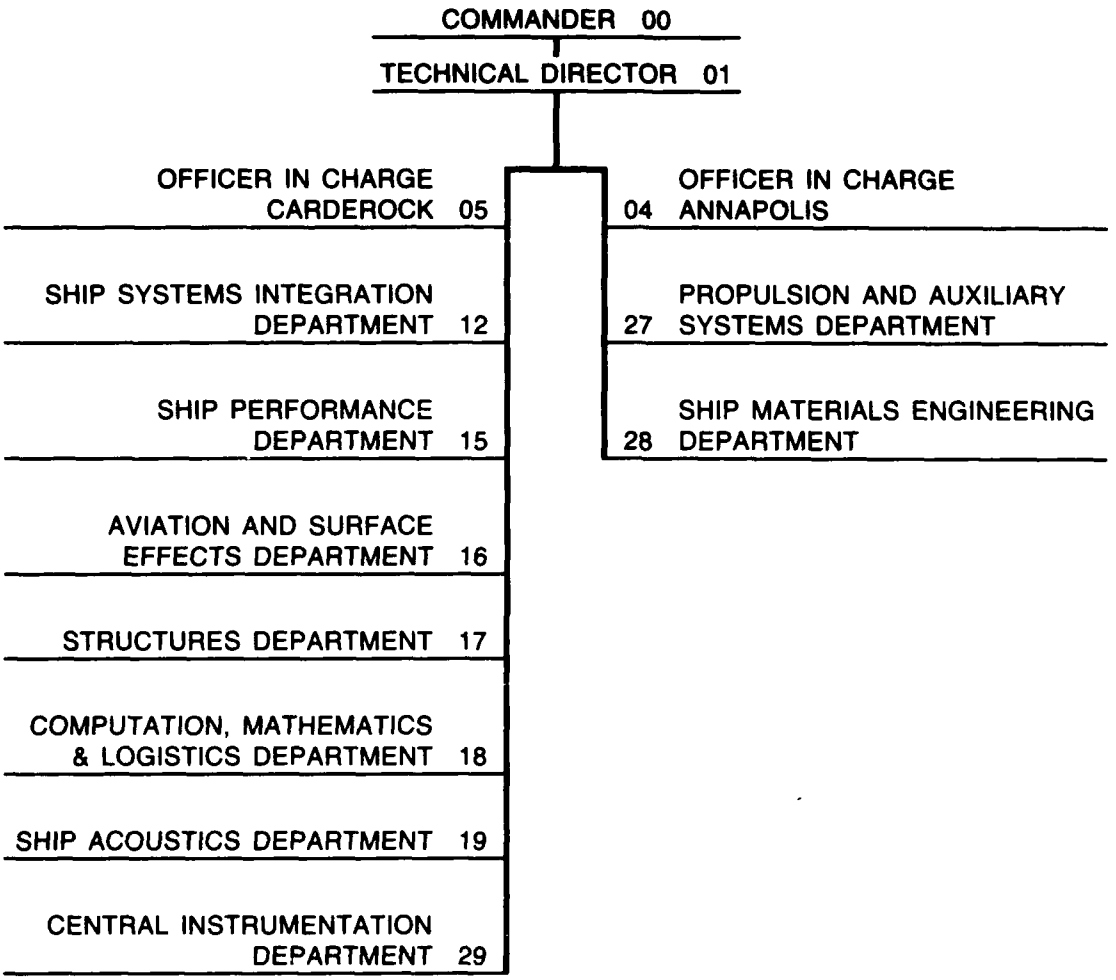

DESTRUCTION NOTICE — For **classified** documents, follow the procedures in DOD 5220.22M, Industrial Security Manual, Section II-9, or DOD 5200.1-R, Information Security Program Regulation, Chapter IX. For **unclassified**, limited documents, destroy by any method that will prevent disclosure of contents or reconstruction of the document.

UNCLASSIFIED
SECURITY CLASSIFICATION OF THIS PAGE

REPORT DOCUMENTATION PAGE

1a. REPORT SECURITY CLASSIFICATION: UNCLASSIFIED	1b. RESTRICTIVE MARKINGS
2a. SECURITY CLASSIFICATION AUTHORITY	3. DISTRIBUTION/AVAILABILITY OF REPORT: STATEMENT A
2b. DECLASSIFICATION/DOWNGRADING SCHEDULE	
4. PERFORMING ORGANIZATION REPORT NUMBER(S): DTRC SHD-1268-01	5. MONITORING ORGANIZATION REPORT NUMBER(S)
6a. NAME OF PERFORMING ORGANIZATION: David Taylor Research Center; 6b. OFFICE SYMBOL (If applicable)	7a. NAME OF MONITORING ORGANIZATION
6c. ADDRESS (City, State, and ZIP Code): Bethesda, Maryland 20084-5000	7b. ADDRESS (City, State, and ZIP Code)
8a. NAME OF FUNDING/SPONSORING ORGANIZATION: Office of Naval Research; 8b. OFFICE SYMBOL (If applicable)	9. PROCUREMENT INSTRUMENT IDENTIFICATION NUMBER
8c. ADDRESS (City, State, and ZIP Code)	10. SOURCE OF FUNDING NUMBERS

PROGRAM ELEMENT NO.	PROJECT NO	TASK NO.	WORK UNIT ACCESSION NO
61153N		B102301N1	DN#507106

11. TITLE (Include Security Classification)

NEAR AND FAR FIELD PROPELLER WAKE STUDY USING LASER DOPPLER VELOCIMETRY

12. PERSONAL AUTHOR(S)
James N. Blanton and Scott Fish

13a. TYPE OF REPORT	13b. TIME COVERED	14. DATE OF REPORT (Year, Month, Day)	15. PAGE COUNT
TECHNICAL	FROM _____ TO _____	JUNE 1988	45

16. SUPPLEMENTARY NOTATION

17. COSATI CODES		
FIELD	GROUP	SUB-GROUP

18. SUBJECT TERMS (Continue on reverse if necessary and identify by block number)
PROPELLER WAKE, LASER DOPPLER VELOCIMETER, FAR WAKE.

19. ABSTRACT (Continue on reverse if necessary and identify by block number)

Two towing tank experiments using a slender boat and a body of revolution model to produce a propeller wake near the free surface were conducted. The first experiment demonstrated the feasibility of the LDV measurement system by utilizing several modes of velocity data collection and correlation in the propeller wake. Mean and blade rate periodic turbulent flow quantities were collected showing good comparison with other published data in the region slightly downstream (< 1 diameter) of the propeller. It was also found that by 5 diameters downstream, the periodicity of the velocity distribution was no longer visible. In the second experiment, streamwise mean velocity measurements were obtained far downstream (18 diameters) of the propeller. Preliminary propeller wake characteristics were measured for the purpose of gaining an understanding of the growth rate and nature of the flow. These
(Continued)

20. DISTRIBUTION/AVAILABILITY OF ABSTRACT	21. ABSTRACT SECURITY CLASSIFICATION
☐ UNCLASSIFIED/UNLIMITED ☒ SAME AS RPT ☐ DTIC USERS	UNCLASSIFIED

22a. NAME OF RESPONSIBLE INDIVIDUAL	22b. TELEPHONE (Include Area Code)	22c. OFFICE SYMBOL
James N. Blanton	(301) 227-1326	Code 1543

DD FORM 1473, 84 MAR — 83 APR edition may be used until exhausted. All other editions are obsolete.

SECURITY CLASSIFICATION OF THIS PAGE
UNCLASSIFIED

(Block 19 Continued)

characteristics could be used to plan a more detailed study of the far-field propeller wake and its interaction with the free surface. Significant propeller wake interaction with the free surface was not observed 18 diameters downstream due to the relatively large propeller submergence depth (1.5 diameters to propeller axis). Axial swirl decay and movement of the center of swirl were also evaluated. Both experiments allowed refinements in seeding methods and LDV implementation which can be utilized for measurements taken closer to the free surface.

CONTENTS

FIGURES

TABLES

NOTATION

C_{TH}	Propeller thrust loading coefficient
D	Propeller diameter
J	Advance ratio ≡ u D/n
n	Propeller rps
r	Radial distance from model axis
R	Propeller radius
U_∞, U_{fs}	Freestream velocity
u,v,w	Axial, transverse and vertical velocity components
v_{tan}	Tangential velocity
x	Streamwise distance
y	Transverse (*across-basin*) *distance*
z	Vertical distance

Greek Symbols

ρ	Density of Fluid

ABSTRACT

Two towing tank experiments using a slender boat and a body of revolution model to produce a propeller wake near the free surface were conducted. The first experiment demonstrated the feasibility of the LDV measurement system by utilizing several modes of velocity data collection and correlation in the propeller wake. Mean and blade rate periodic turbulent flow quantities were collected showing good comparison with other published data in the region slightly downstream (< 1 diameter) of the propeller. It was also found that by 5 diameters downstream, the periodicity of the velocity distribution was no longer visible. In the second experiment, streamwise mean velocity measurements were obtained far downstream (18 diameters) of the propeller. Preliminary propeller wake characteristics were measured for the purpose of gaining an understanding of the growth rate and nature of the flow. These characteristics could be used to plan a more detailed study of the far-field propeller wake and its interaction with the free surface. Significant propeller wake interaction with the free surface was not observed 18 diameters downstream due to the relatively large propeller submergence depth (1.5 diameters to propeller axis). Axial swirl decay and movement of the center of swirl were also evaluated. Both experiments allowed refinements in seeding methods and LDV implementation which can be utilized for measurements taken closer to the free surface.

ADMINISTRATIVE INFORMATION

The work described in this report is part of the Surface Ship Wake Consortium sponsored by the Office of Naval Research (ONR) Applied Research Program, under Program Element 61153N, Task Area BT02301N1, and performed under the David Taylor Research Center (DTRC) work units 1-1543-128 (FY 87) and 1-1504-200 (FY 88).

INTRODUCTION

Over the last decade, the use of synthetic aperture radar in oceanographic satellites has revealed interesting backscatter images of oceanic flow phenomena and ship wakes. One characteristic feature of these images, a narrow dark scar centered in the track behind a moving ship, has been of particular importance in the field of ship signatures. It has been

postulated that the dark region is caused by the influence of the turbulent wake of the ship on the Bragg scattering of radar signals at the free surface (Lyden et.al, 1985). The physics of this interaction process is not well understood due to limited knowledge of the turbulent interaction phenomena for even very simple wake models. In order to develop an understanding of the wake interaction with the free surface and to provide guidance for computer modelling of wake/free surface simulators, a three phase experimental investigation was initiated to characterize the interaction of propeller wake and turbulence (a major source for the typical ship) with a free surface. An additional incentive for this study was the carryover of this understanding to designers in pursuit of propellers which could either reduce the "scar" size or in some way change its character.

During the first phase, which is reported herein, feasibility tests were conducted using Laser Doppler Velocimetry (LDV) equipment to measure the propeller wake both far downstream and near the free surface. In addition, a cursory survey of the far wake of a propeller was conducted to characterize the flow evolution and highlight any difficulties to be overcome in detailed measurements in subsequent phases of the investigation. Two towing tank experiments using a slender boat and a body of revolution model were conducted. The first experiment demonstrated the feasibility of the LDV measurement system by utilizing several modes of velocity data collection and correlation in the propeller wake. Mean and blade rate periodic turbulent flow quantities were collected showing good comparison with published data in the region slightly downstream (< 1 diameter) of the propeller. In the second experiment, streamwise mean velocity profiles were obtained far downstream (up to 18 diameters) of the propeller. Preliminary propeller wake

characteristics were measured for the purpose of both gaining an understanding of the growth rate and nature of the flow and providing coarse empirical data sets for comparison with numerical simulation results. These characteristics could be used to plan a more detailed study of the far downstream propeller wake and its interaction with a free surface. A transverse velocity survey was obtained at several axial positions for use in propeller wake prediction codes under development at NRL by Swean (1987). Both experiments led to refinements in seeding methods and LDV implementation which can be utilized for measurements taken closer to the free surface.

The later phases of the investigation will be discussed in the conclusions section of this report.

EXPERIMENTAL FACILITIES

TOW TANK AND CARRIAGE

The DTRC Carriage 1 towing basin was used for the experiments presented in this report. Carriage velocity was maintained at two knots (1.024 m/s) for all runs. This constraint to one speed was chosen for the purpose of obtaining, in the limited time and budget, a more complete data set for comparison with numerical results.

MODELS AND PROPELLERS

Two models and three propellers were used in these experiments. The first model, DTRC Propeller Boat (Figure 1a), was outfitted with a three bladed, 12 inch diameter propeller. After velocity surveys were made at several axial distances, the Propeller Boat was replaced with a submerged body of revolution model (DTRC model #4627) supported by two struts (Figure 1b). The length and

maximum diameter of this model were 15.1 ft. (4.6 m) long and 1.9 ft (0.58 m). The model change reduced both the circumferential non-uniformity in inflow velocity to the propeller and the free surface disturbance in the wake region. These two changes were required for greater similarity with the boundary conditions used in numerical simulations being conducted by Swean (1987). The model was attached to the carriage girder. The distance from the propeller to the measurement position was varied by LDV traverse motion (approximately 1.7 D travel) and by attaching the model at different positions along the girder (approximately 20 D travel). Two 10.8 inch (27.4 cm) diameter five bladed propellers were used with this model. Although both propellers were designed for the same open water performance, one (DTRC #3666) had blades of approximately 20 percent larger chord than the other (DTRC # 3667). Propeller #3666 was operated at C_{TH} approximately 1.2 (J_T = 0.58) and propeller #3667 operated at C_{TH} approximately 1.4 (J_T = 0.58) (See Appendix B). The design condition for propeller #3666 was J = 0.610 and for propeller #3667 was J = 0.636. The propeller centerline was positioned at 1.65 D below the free-surface.

LASER DOPPLER VELOCIMETER SYSTEM

Velocity measurements were taken using a TSI two-component fiber-optic Laser Doppler Velocimeter (LDV). This system consisted of a 4W argon-ion laser, frequency shifters, and counter type signal processors. The final transmitting and receiving lenses were located in a fiber-optic "probe". The "probe" was mounted on the end of a strut downstream of the propeller (see Figure 2). A three-dimensional traversing mechanism allowed travel of 18 inches (45.72 cm) in both x and z, and 36 inches (91.44 cm) in y.

Data was collected using an IBM compatible micro-computer using data acquisition equipment and techniques developed by Fry et al. (1987). Data was then transferred to an Apollo workstation and an IDM compatible micro-computer for analysis and graphics output.

SEEDING

Several seeding methods were tried in this study with the aim of maximizing seed detections in the measurement volume and minimizing the flow disturbance due to the seeding method itself. The flow was seeded using a slurry of 4-10 micron silver coated glass beads in water. The high cost of this seed prohibited the use of very large quantities to saturate the basin. The slurry was therefore introduced into the flow only in the region upstream of the propeller.

When using the Propeller Boat, seed was injected from 16 tubes mounted concentrically around the shaft upstream of the propeller (see Figure 1a). This method of seeding gave data rates between 100 and 400 counts per second in the propeller wake depending on radial location of the probe.

When using the body of revolution model, seed injected from sixteen holes circumferentially spaced forward on the hull did not disperse beyond a two inch radius at the propeller plane. This trapping of the seed in the boundary layer could not give adequate data rates beyond r/R of 0.5. Little success was found in spraying the seed on the free surface prior to a basin run. Seed was therefore injected far upstream (approximately 40 propeller diameters forward of the measurement volume) from nozzles on a circular pipe. (Note: The distance from the seeding strut to the propeller varied with model girder position. See Figure 1). Vortex shedding from the seeding pipe encouraged seed dispersal in the flow but also contributed to unsteady inflow to the

propeller. A faired strut was therefore drilled as shown in Figure 1 to provide ample seed dispersion with minimal wake effect on the propeller.

Data rates typically varied from 50 to 300 counts per second in the propeller race. At the edge and outside of the race data rates as low as 5–10 counts per second were encountered. The resulting low rates of seed detection created difficulties in determining the velocities in the irrotational regions of the flow. More detailed study of propeller wakes with the LDV system will require additions to the current seeding method to increase transverse seed dispersal.

VELOCITY DATA COLLECTION MODES

SHAFT RATE SYNCHRONIZED MODE

Velocity measurements synchronized with propeller position were made to demonstrate measurement feasibility using the LDV. A once per revolution pulse generated by a magnetic pick–up reset a shaft position counter each revolution. Velocity signals measured by the LDV system were then stored and ensemble averaged according to the counter readout at the time of the measurement.

The distribution of averaged velocity over all the counter values gave an ensemble averaged picture of the velocity at the point of measurement due to flow effects corresponding to propeller position. This technique has been previously used to measure blade rate characteristics of propeller wakes (Min (1978), Kotb and Schetz (1984), Jessup et al. (1985), Nagle and McMahon (1985), Wang (1985), and Blaurock and Lammers (1986)). Bumps and deficits, which correspond to the wake of each propeller blade, can be located in these velocity distributions.

TIME AVERAGE MODE

Mean velocity measurements were taken at distances from x/D = 0.6 to x/D = 18.0. Because only two components of velocity were measurable at a time, two probe orientations were utilized to obtain three velocity components. Figure 2 shows the body of the probe mounted in the two orientations used for this experiment. The orientation perpendicular to the axis of the model measured streamwise (u) and vertical (v) velocities. The orientation parallel to the model axis measured vertical (v) and transverse (w) velocities.

COINCIDENT UV MODE

Velocity measurements were also taken in the coincident mode. To obtain a valid velocity data point, two measurements (one from each component) must be obtained within a coincident time window. This measurement can, with high data rates, allow determination of Reynolds stress. Coincidence mode data rates during this experiment (for a coincidence window of approximately 1 ms) decreased significantly over random mode measurements. The excessive test time required for these measurements was therefore not pursued beyond a feasibility validation.

RESULTS AND DISCUSSION

LDV FEASIBILITY

The fiber optic LDV is very well suited for propeller wake velocity measurement of this type. This LDV requires no calibration and minimizes flow disturbances (see Appendix A). In addition, the final transmitting and receiving optics are small and light enough to be easily traversed. For this experiment, seeding difficulties (see SEEDING section) were resolved to obtain sufficiently high rates of data collection. The precision uncertainty for the

LDV was determined to be 0.6 percent by repeated measurements. Repeatability measurements are outlined in Appendix A.

Figures 3a and 3b show typical blade rate velocity plots collected on the three bladed propeller. The shapes and sizes of the blade wake bumps in these plots correlate well with similar measurements by Blaurock and Lammer (1986) demonstrating the feasibility of the LDV system in a synchronized blade rate data collection mode.

BLADE RATE ANALYSIS OF FIVE BLADED PROPELLER

Using the body of revolution model and the five bladed propeller (DTRC #3667) measurements of blade rate velocities were made at several axial and radial locations. Analysis of these synchronized velocity measurements is given in this section.

Axial Velocity

Figure 4 shows radial variations in the synchronized axial velocity at different axial locations in the wake. At x/D=0.5 (Figure 4a) five velocity deficits can be seen in the angular profile for r/R=0.2. These deficits correspond to the wake of each blade. The second deficit from the left, however, does not have as large a deficit as the others. As r/R is increased to 0.5 in Figure 4a the angular spacing of the deficits is affected near the anomaly. At r/R=0.8 the characteristic peak in velocity profile caused by the tip vortex actually reverses and becomes a deficit, indicating a negative loading on this second blade near the tip. Measurements of the propeller geometry suggest that this second blade corresponded to blade #4 marked on the propeller (see Figure 5). It should be noted that the out-of-tolerance of the

odd blade was small enough to be visible only after the blade was identified by these measurements.

Further downstream, Figures 4b and 4c show a loss of blade rate velocity dependence and a growth of velocity dependence in shaft frequency. Figure 4b indicates a weak dependence on five wake structures at r/R=0.7. Closer to the edge of the wake in the tip vortex region, one large characteristic bump has formed in the velocity profile. The helix asymmetry caused by the oddly loaded blade apparently accelerates the destruction of blade rate dependence and gives rise to a growth in dependence on shaft rate. One explanation for this may be the amalgamation of several tip vortex wake structures into one spiraling structure. This merging process could occur under the asymmetric induced velocity field set up by this propeller. Figure 4c shows, at x/D=5.0, only a small velocity variation inside the wake jet of the same period as the shaft rotation. Axial velocity dependence on shaft rate has obviously persisted much farther downstream than the blade rate dependence in this case of asymmetric propeller loading.

Tangential Velocity

Figures 6a and 6b show tangential blade-rate velocity profiles. These profiles agree with Figures 4a, 4b and 4c in showing asymmetric loading for one blade. Again, by x/D=2.0 the blade rate dependence has diminished and is replaced (especially nearer the wake centerline) by a shaft rate oscillation.

Radial Velocity

Figure 7 shows radial blade-rate velocity profiles. These figures also agree with the previous figures in showing the shift from blade rate dependence to shaft rate dependence. Incorrect settings on the LDV system

prohibited use of data collected at x/D=0.5. Note also that spacial variations in radial velocity inside the jet wake show a stronger influence on spacial variations outside the wake when compared to tangential velocity variations. Comparison of velocity profiles at r/R=0.74 with r/R=1.1 in Figures 6b and 7b illustrate this difference.

TIME AVERAGED PROPELLER WAKE

The body of revolution model was used for mean velocity measurements. Propeller #3666 was used for all mean velocity measurements due to the defect observed in blade rate velocity plots of propeller #3667 (See BLADE RATE ANALYSIS OF FIVE BLADED PROPELLER section).

Mean Velocity Profiles

Figure 8 shows mean axial velocity profiles for x/D ranging from 0.6 to 18.0. Each profile is taken at z=0.0. The jet decay can easily be seen in this figure accompanied by the classic jet spreading. Further discussion of the spreading is covered in the Wake Radius Evolution section.

One feature observed near the propeller in both vertical and transverse profiles was a local peak in axial velocity at the hub. This feature could be caused by secondary flows originating at the hub–blade intersection. Horseshoe vortices created at this intersection form streamwise vorticity in the hub region. This streamwise vorticity may transfer high momentum fluid into the hub–wake region causing a local peak in axial velocity at the hub.

Wake Radius Evolution

Evolution of the propeller wake radius is shown in Figure 9. For positions greater than 2 diameters downstream, only measurements in the negative y direction (y–) corresponding to the starboard side of the model contained enough information to determine the edge of the propeller wake.

Measurements for axial positions less than 2 diameters for positive y (y+) and positive z (z+) show good agreement with y−. Calculations for positive z (z+) were not made due to distortion of the propeller wake caused by the support strut wake. The procedure for determining the wake edge first involved determining an average value for mean streamwise (U) velocity in the "free-stream" outside the propeller wake. Determination of which points "belong" to the freestream averaging group was made by marching inward (toward the propeller centerline) from the outer velocity measurements and including the next point if its value was within the 2 standard deviations calculated for the previous points. Figures 10a and 10b show typical near field wake and far field wake profiles. The edge axial velocity was defined to be 101 percent of the freestream value. To determine the wake edge position, an interpolation was performed between the first free-stream point and the first point inside the wake. Further downstream the velocity profile exhibits a shallower slope which increases the uncertainty of determining the 2 standard deviations cutoff and resulting edge of the wake.

The displacement of the center of swirl from the x axis adds uncertainty in determining the wake radius because both edges were not measurable farther aft in the wake (See Figure 8).

Transverse Mean Velocity Survey

Figures 11-13 show transverse velocity vectors at x/D = 5.0, 7.5, and 10.0. Each radial and tangential point is an average of 1024 individual LDV data points. Each complete grid took approximately 15 carriage passes. The decay of swirl from 5 to 10 diameters downstream can be qualitatively observed. Figure 14 shows the free-surface in relation to transverse velocity

vectors at x/D = 10. The vertical extent of the propeller wake at x/D = 10 is about 0.5 propeller diameters beneath the free-surface.

Swirl Calculation

Propeller wake calculation codes being developed at NRL characterize the wake by its swirl. Calculations were performed on the data for verification of the swirl decay in the propeller wake. The quantities calculated are given below:

$$\text{swirl rate} = 2\pi \int_0^\infty \rho\, u(r)\, v_{tan}(r)\, r\, dr$$

$$\text{swirl number} = \frac{\text{swirl rate}}{2\pi \int_0^\infty \rho\, U_\infty^2\, r\, dr}$$

The local axial and tangential velocities were extracted from data along the y axis (z=0) at various axial distances downstream. Cubic splines were then fit to the data to obtain smooth profiles in the peaking regions of the velocity before integration was performed. Figure 15 shows the decreasing trend in the data with increasing axial location. Fluctuations in the swirl quantities in regions where fine axial spacing was measured are indications of the uncertainty band on calculations of this type. The major source of uncertainty was the accurate location of the center of rotation; estimated in this case by finding the zero crossing location of the tangential velocity.

CONCLUSIONS

The fiber optic two—component LDV system showed promise for non—intrusive measurements far downstream in the propeller wake. Blade rate velocity profiles obtained have been compared to data found in the literature. By five diameters downstream of the propeller, the velocity dependance on blade rate is no longer visible. Verification of this phenomenon is currently not possible due to unavailability of other experimental data. The LDV technique also allowed determination of the asymmetric loading on the propeller blades caused by a geometric defect at the tip. Careful measurement of propeller geometry prior to testing is suggested to avoid this type of wake asymmetry.

Mean axial velocity profiles were obtained from $x/D = 0.6$ to 18 diameters downstream of the propeller allowing determination of the propeller wake radius evolution. Transverse mean velocity vector plots were obtained at three axial locations allowing qualitative determination of swirl decay.

With the model located as close to the free surface as possible while minimizing the surface deformation, a long wake examination length without influence of the free surface (with the possibility of a wake intersection with the free surface near the far edge of the measuring space) was obtained. Elimination of possible free surface influences near the propeller allowed swirl properties to be measured for verification of prediction codes being developed at NRL. Wake evolution properties could also be evaluated for later comparison with measurements under the influence of the free surface. In addition, the results of this experiment showed instabilities in the blade rate wake which could easily have been mistaken for free surface effects had the model been located closer to the surface.

The illumination of complicated geometrical instability in the propeller wake by the velocity measurements indicates a need for a more visual perspective on the wake evolution prior to more detailed velocity measurements. Later phases of the investigation should therefore focus on gaining more characteristic insight into the wake structure using flow visualization before returning to the quantitative use of the fiber optic LDV system. Plans are currently being executed for a visualization experiment of the propeller tip vortex structures using dye injection and a laser light sheet.

ACKNOWLEDGEMENTS

The authors gratefully acknowledge the help of Robert Mellish for his contributions in planning and running the experiment and David Fry for his tireless assistance in setting up the LDV. The authors also acknowledge the help of John Hamilton and Yong Kim for their support in running the experiment.

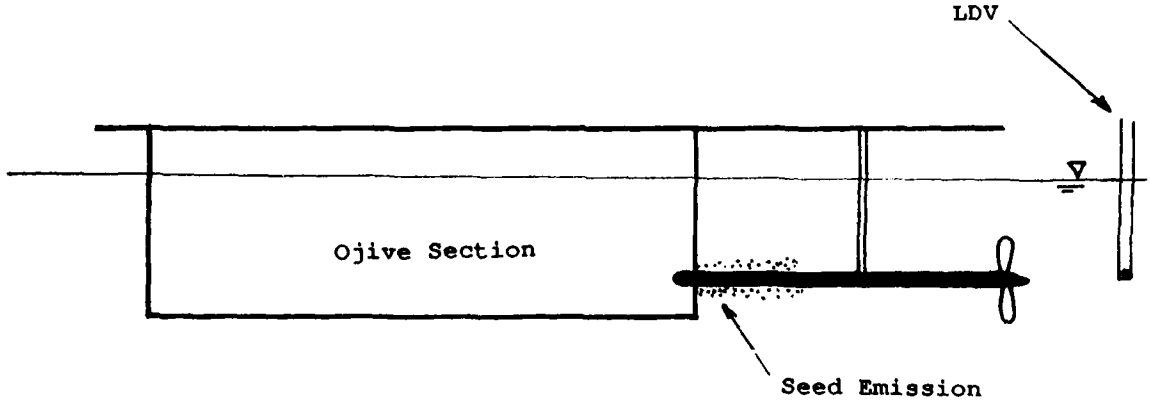

Figure 1a. DTRC Propeller Boat

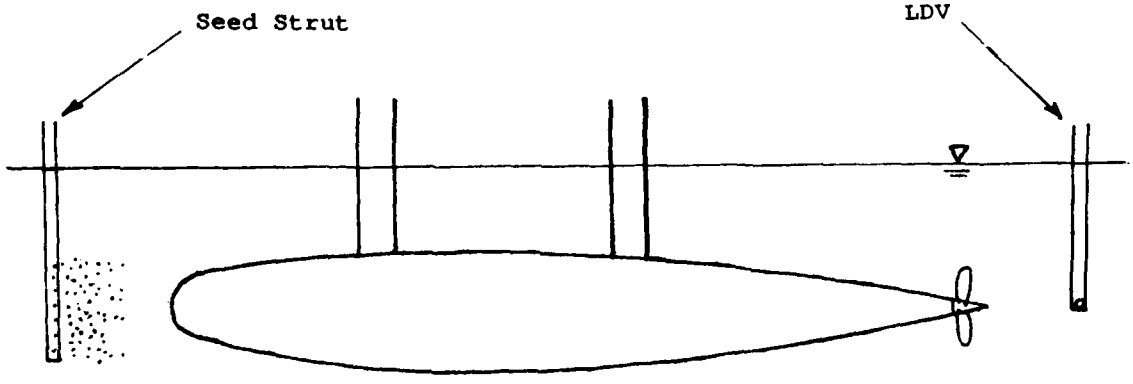

Figure 1b. Body of Revolution Model
Figure 1. Experimental Models

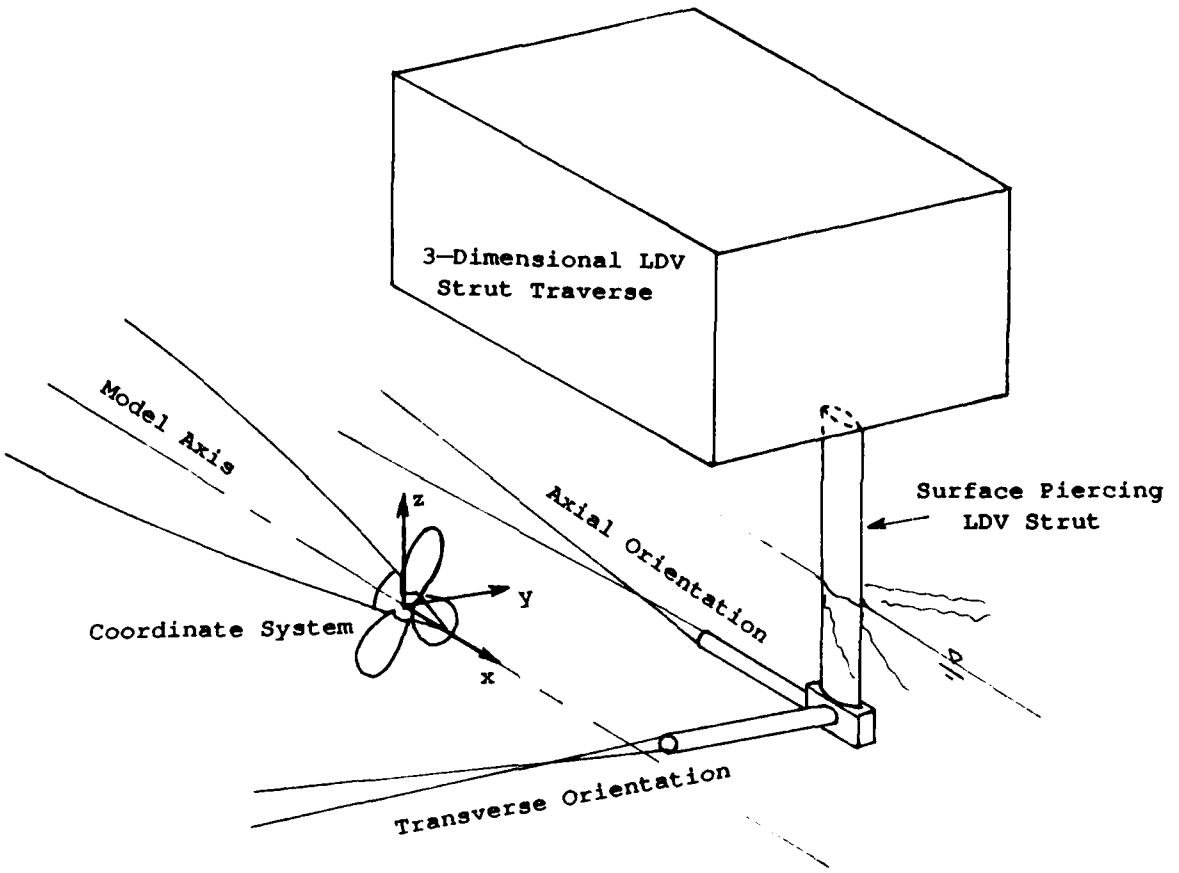

Figure 2. LDV fiber optic probe and support strut

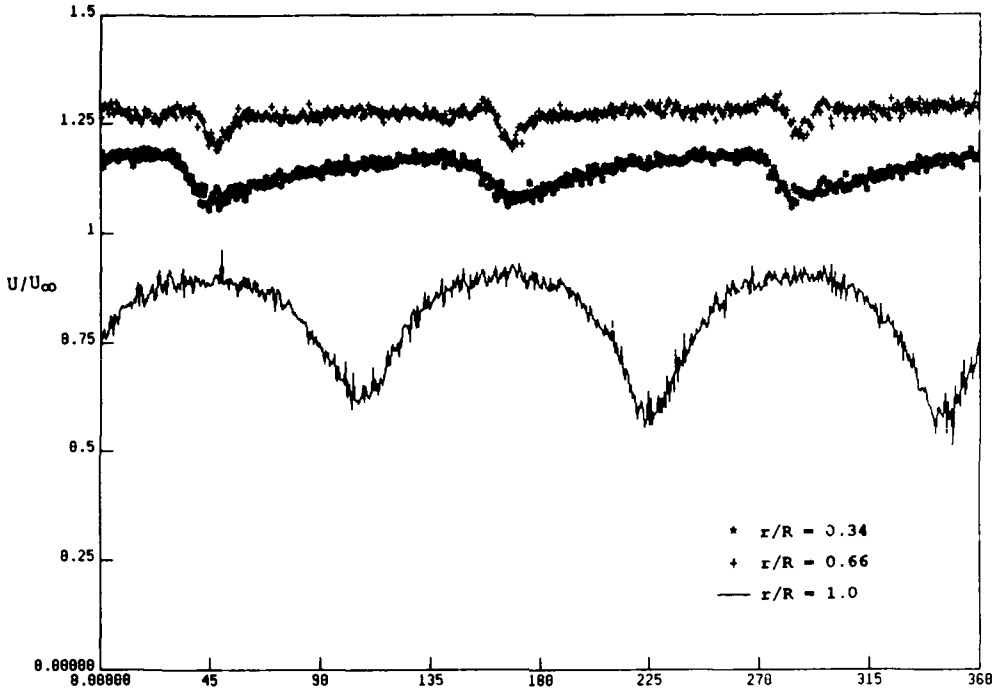

Figure 3a. Axial velocity, x/D = 0.5

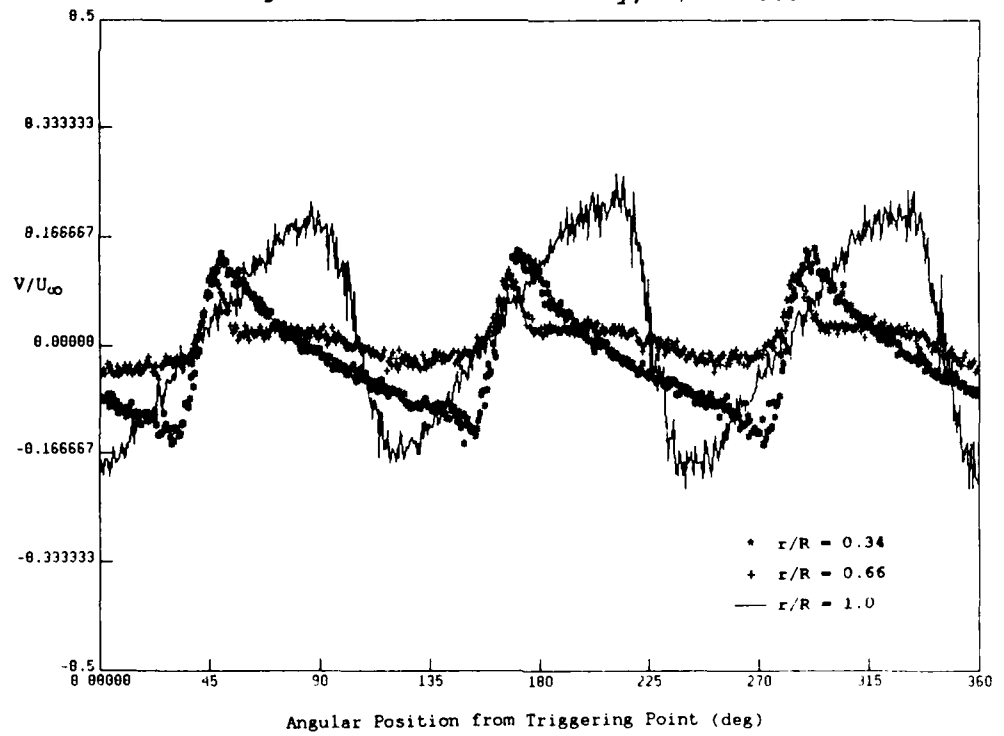

Figure 3b. Radial velocity, x/D = 0.5

Figure 3. Typical blade-rate velocity plots: Three bladed propeller

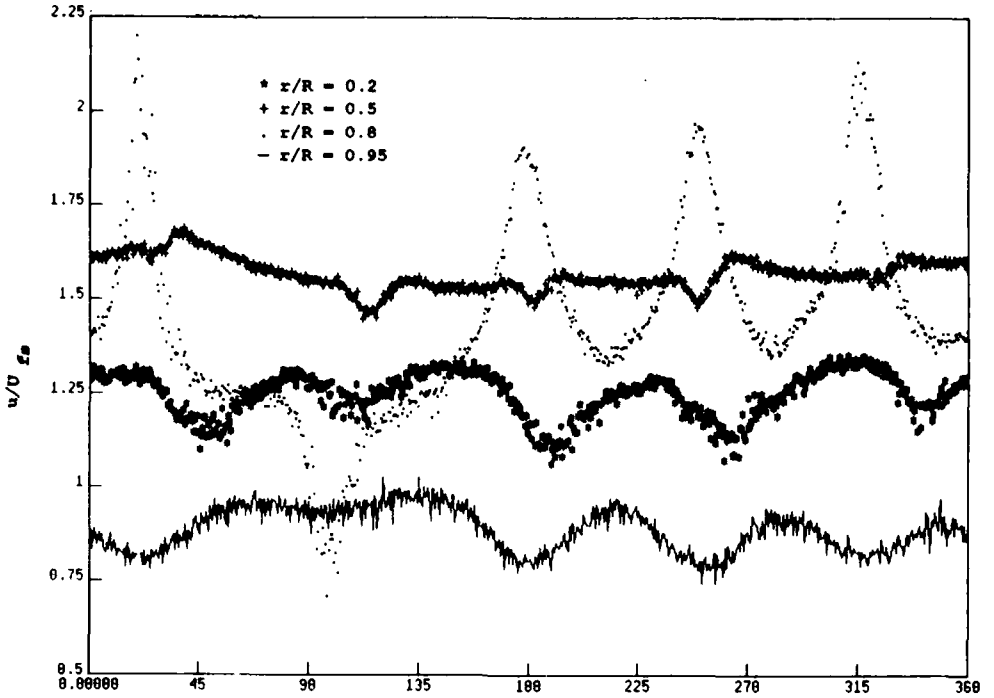

Figure 4a. x/D = 0.5

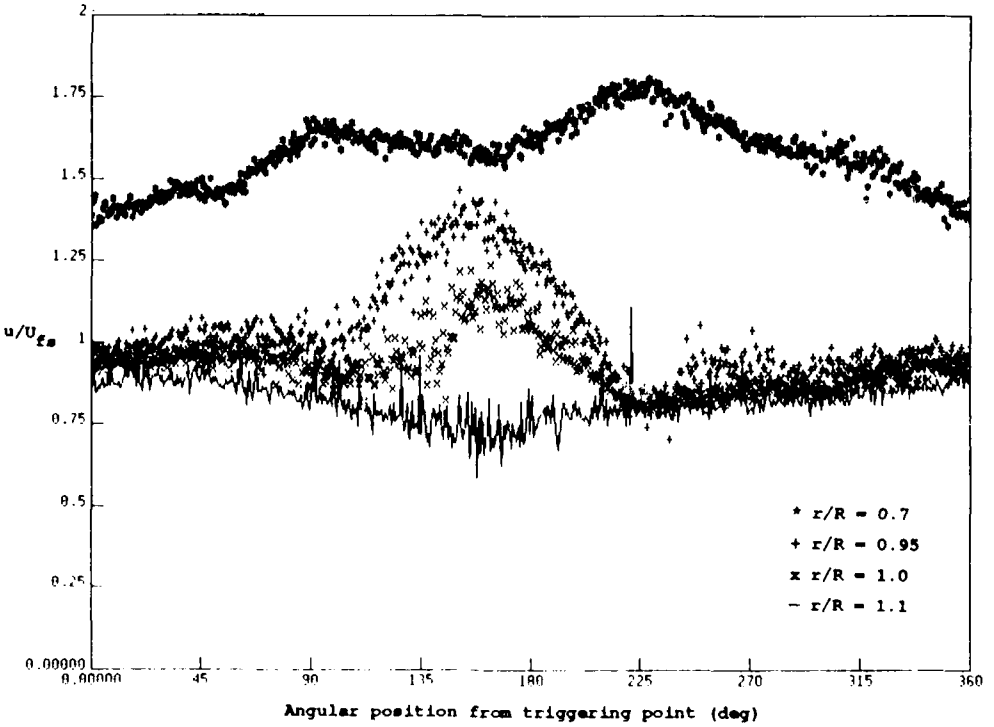

Figure 4b. x/D = 1.25

Figure 4. Axial blade-rate velocity: Five bladed propeller

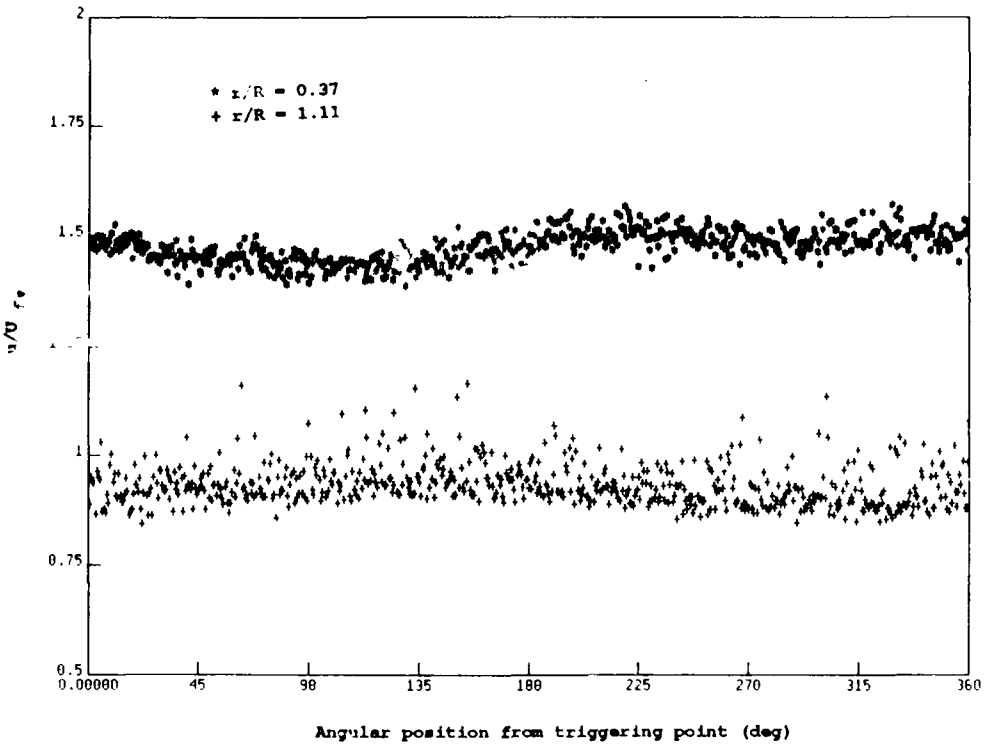

Figure 4c. x/D = 4.8

Figure 4. (Continued)

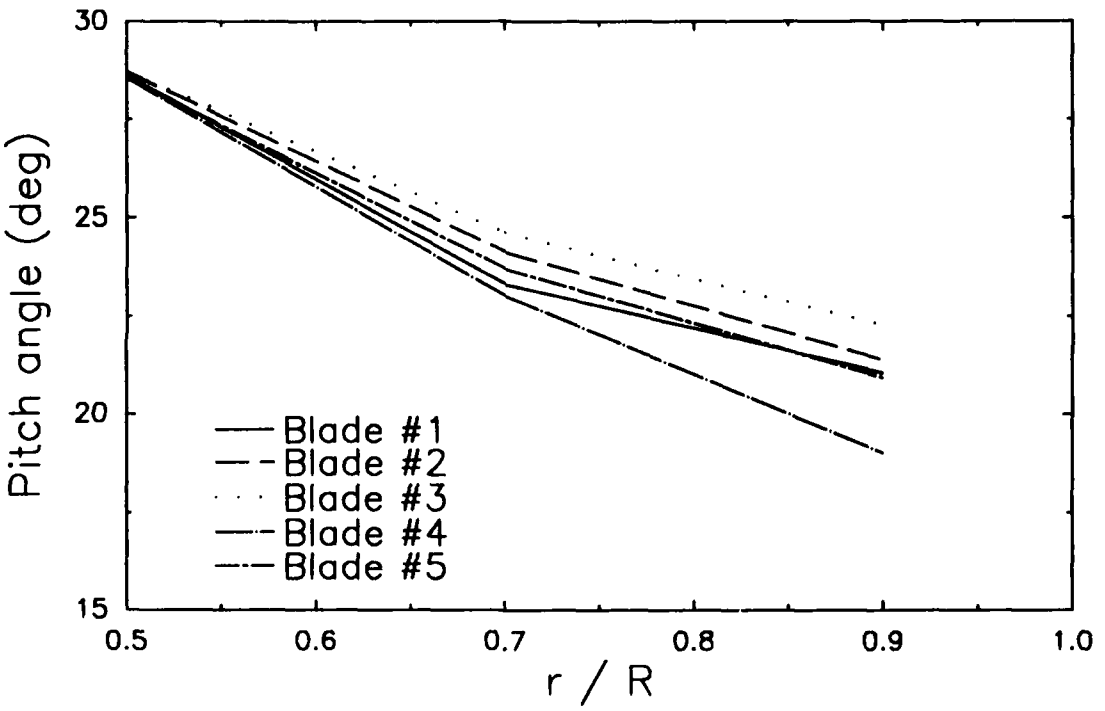

Figure 5. Dimensional measurements on propeller #3667

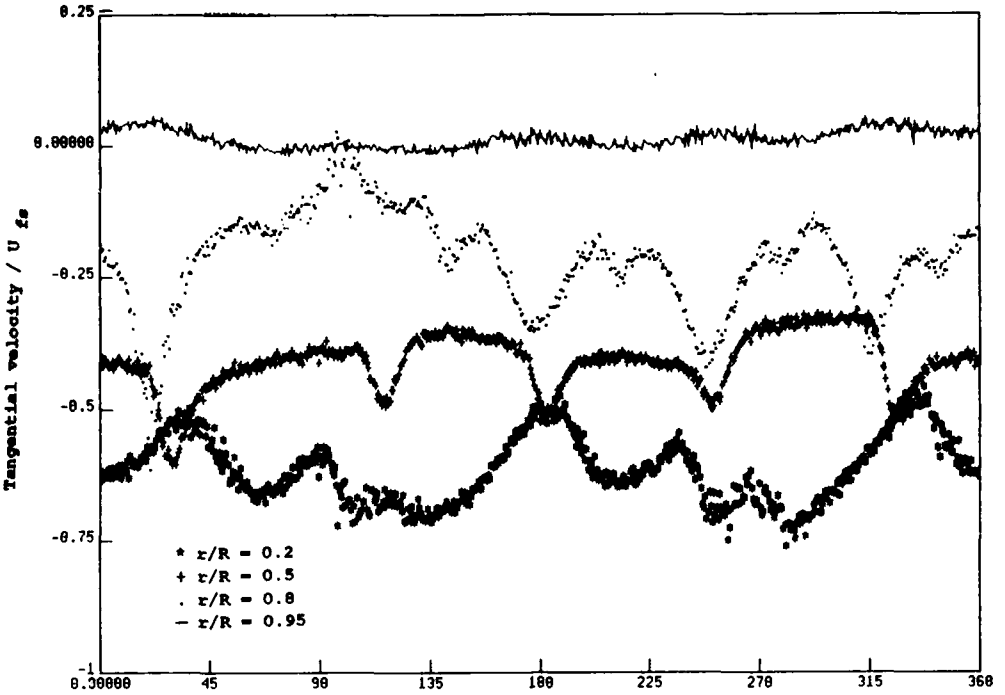

Figure 6a. x/D = 0.5

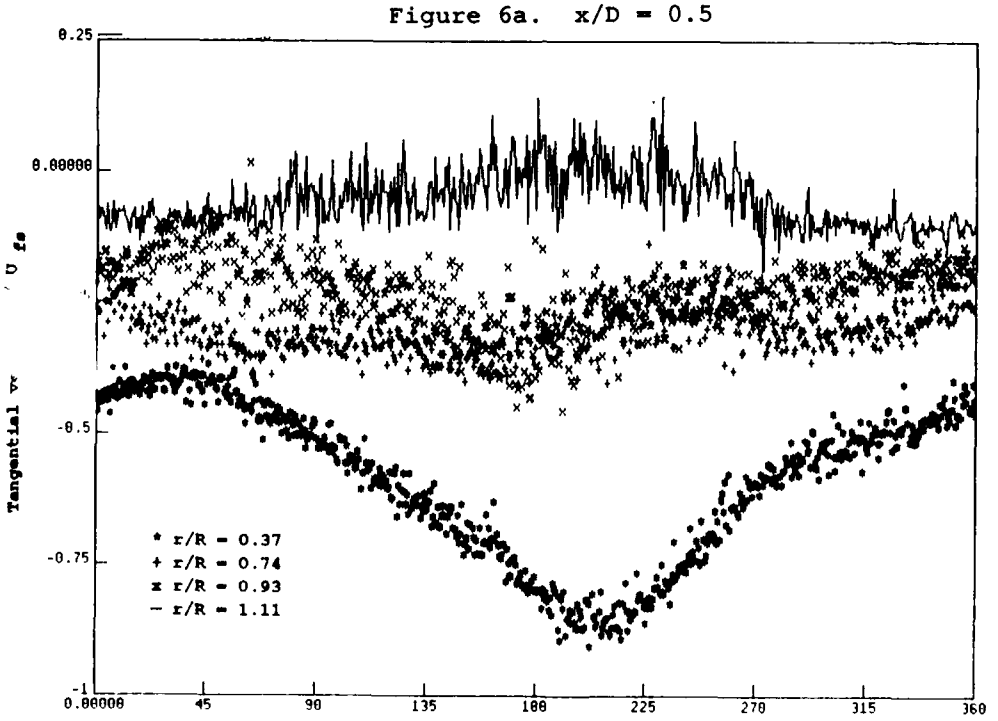

Figure 6b. x/D = 2.0

Figure 6. Tangential blade-rate velocity: Five bladed propeller

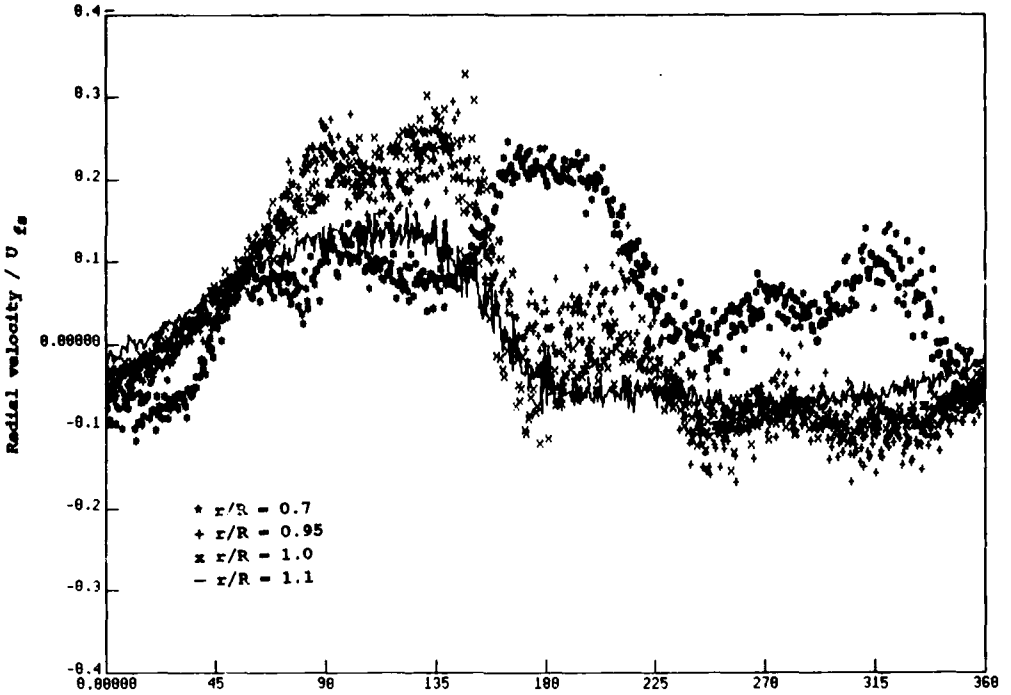

Figure 7a. x/D = 1.25

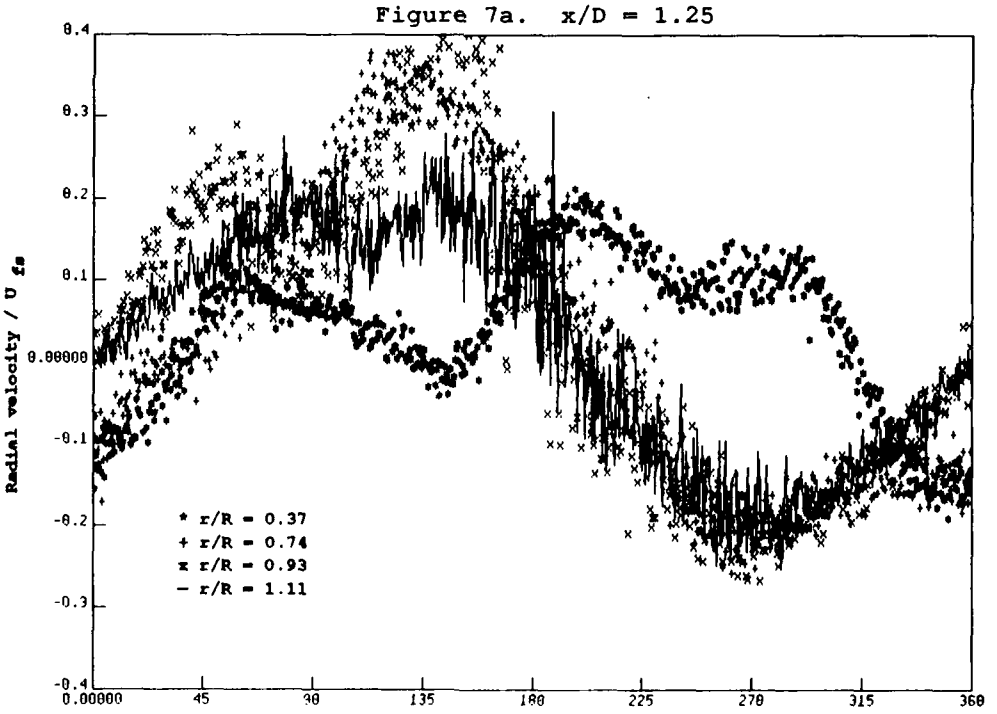

Figure 7b. x/D = 2.0

Figure 7. Radial blade-rate velocity: Five bladed propeller

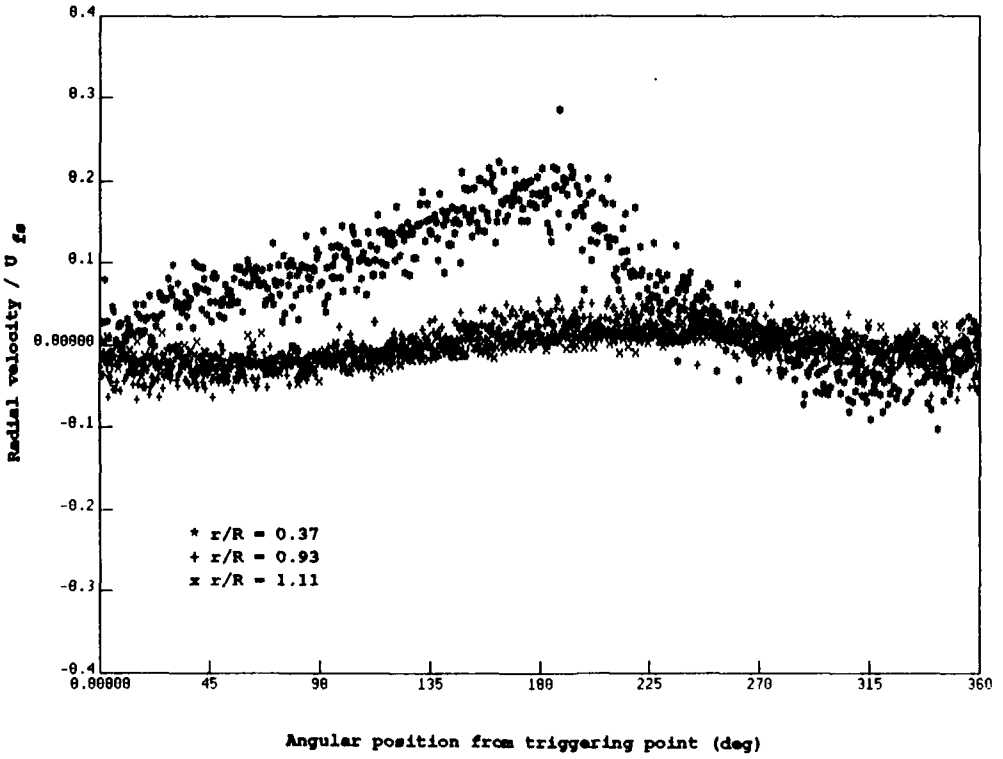

Figure 7c. x/D = 4.8

Figure 7. (Continued)

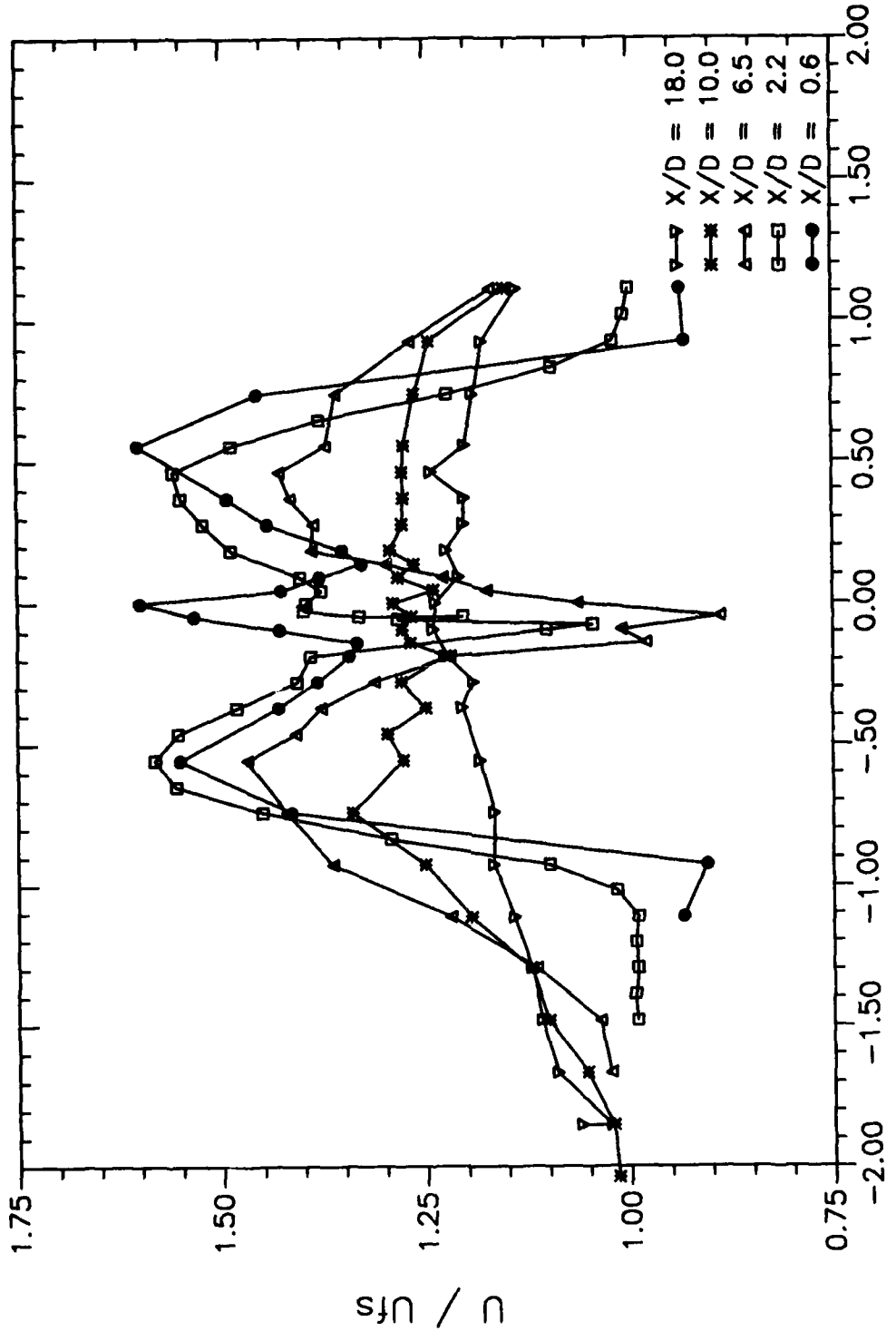

Figure 8. Mean axial velocity, x/D = 0.6 to 18.0

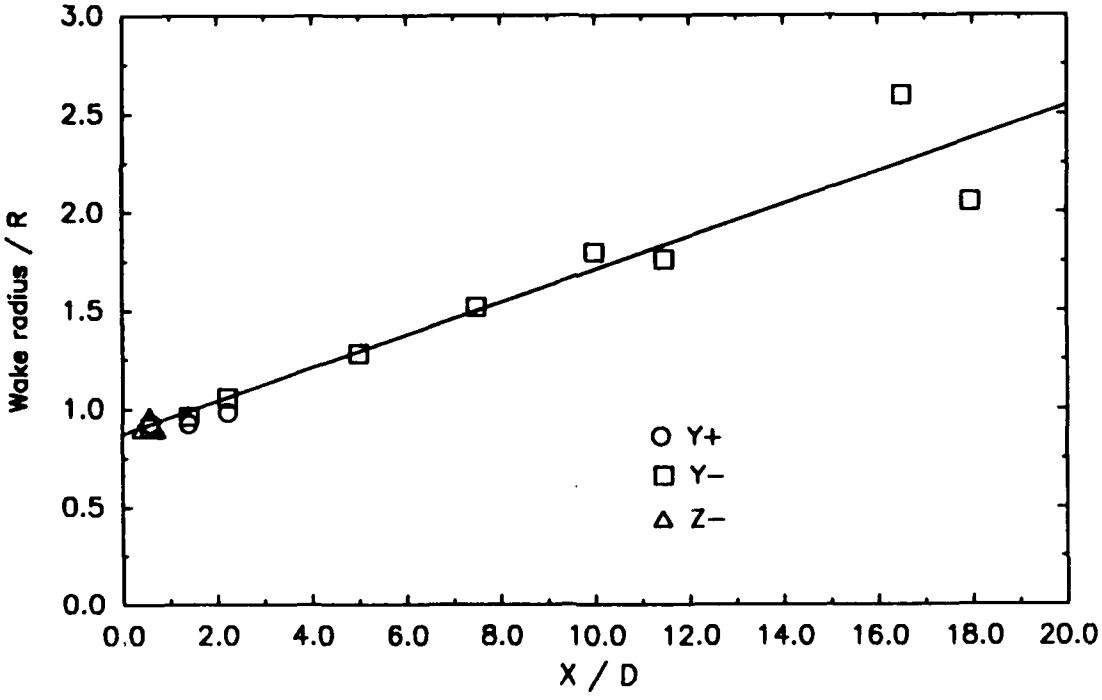

Figure 9. Propeller wake radius evolution

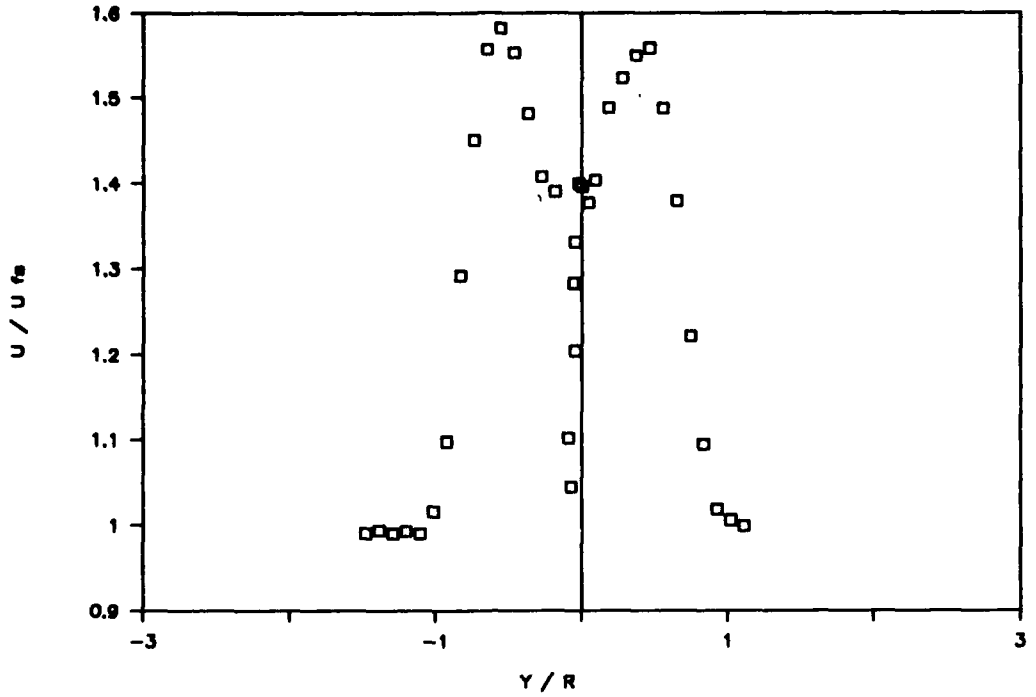

Figure 10a. Near field wake, x/D = 2.2

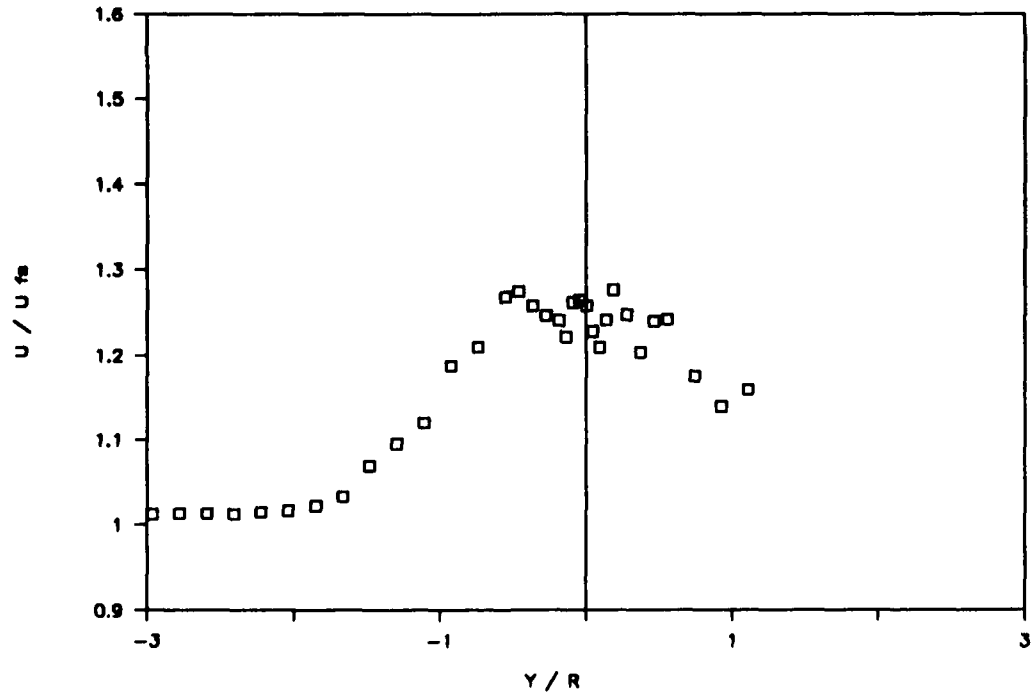

Figure 10b. Far field wake, x/D = 11.5
Figure 10. Typical propeller wake profiles

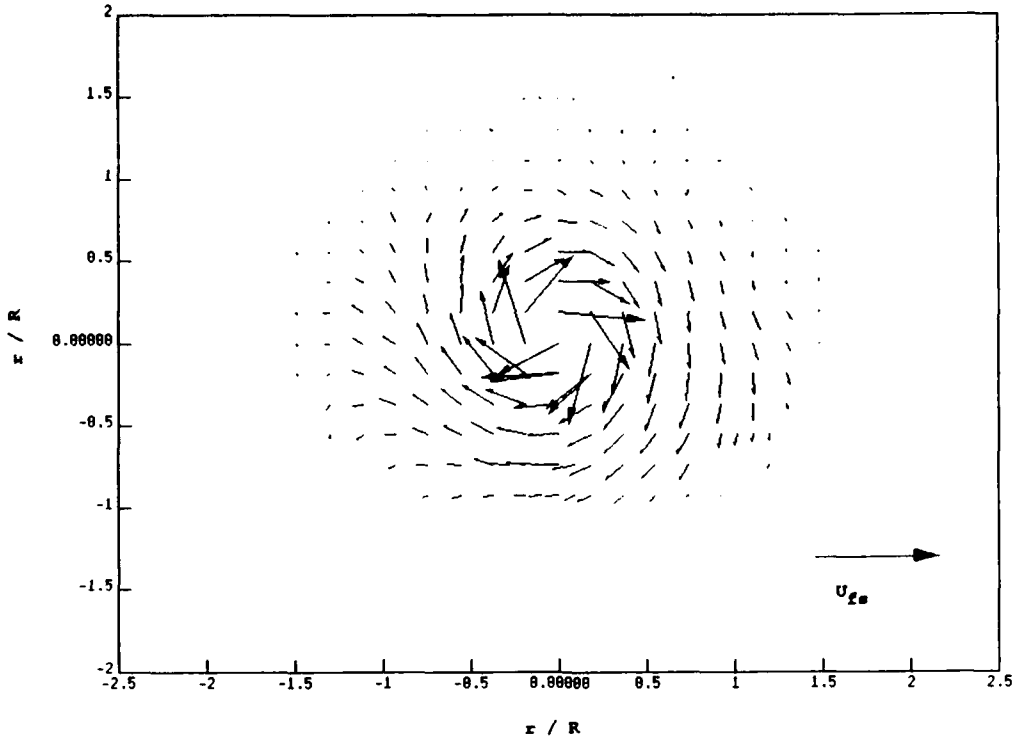

Figure 11. Plot of transverse velocity vectors, x/D = 5.0

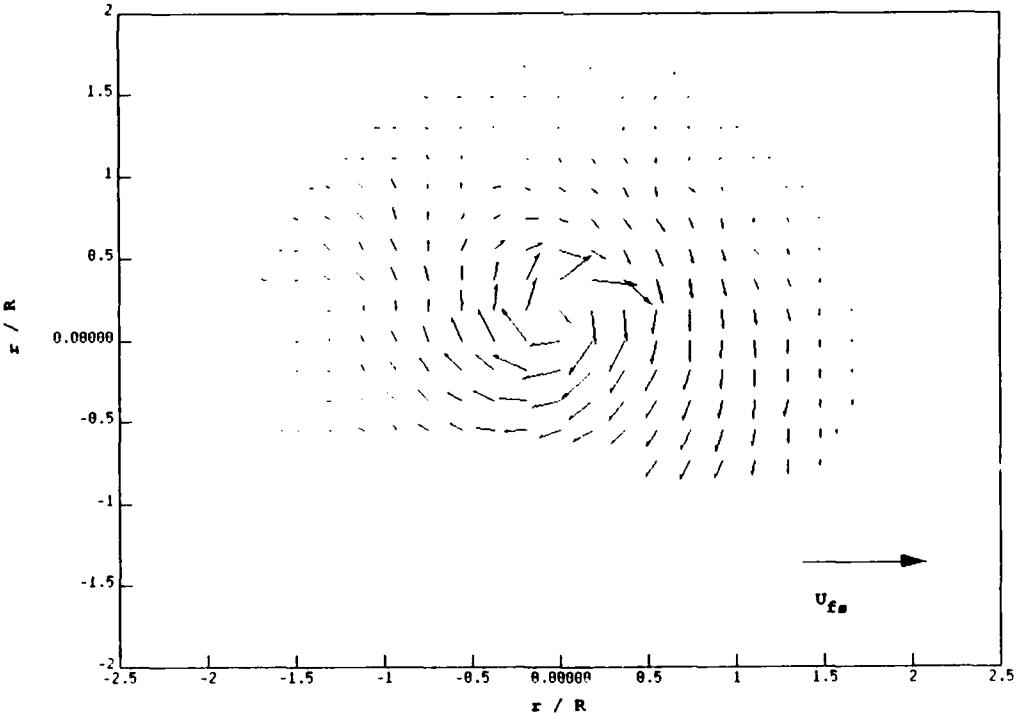

Figure 12. Plot of transverse velocity vectors, x/D = 7.5

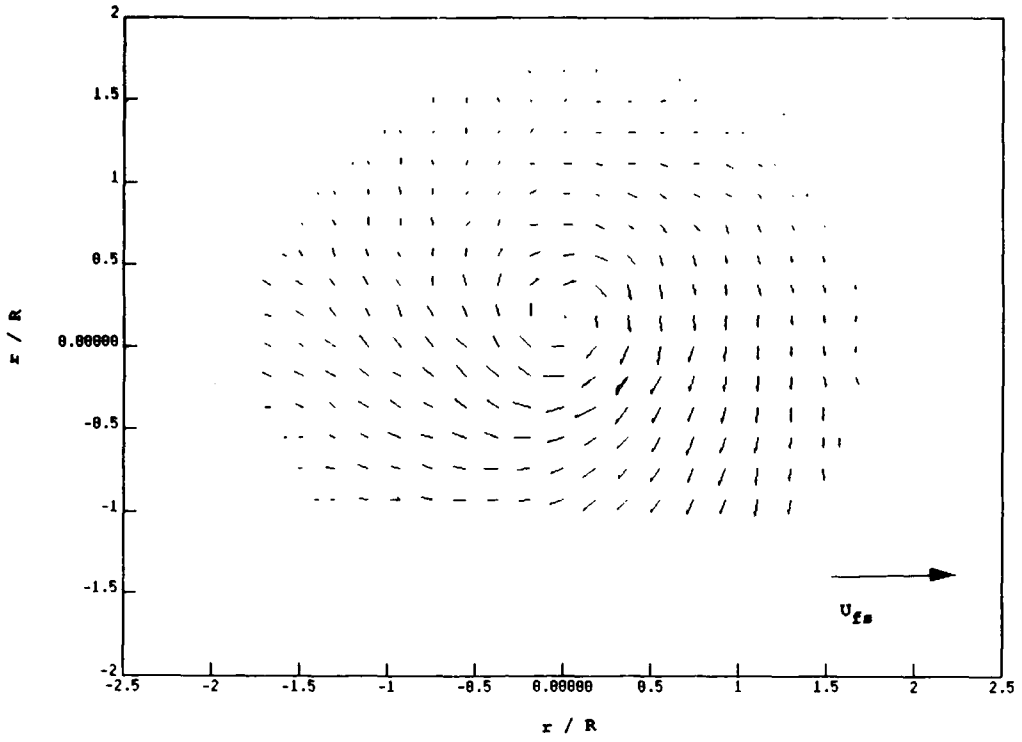

Figure 13. Plot of transverse velocity vectors, x/D = 10.0

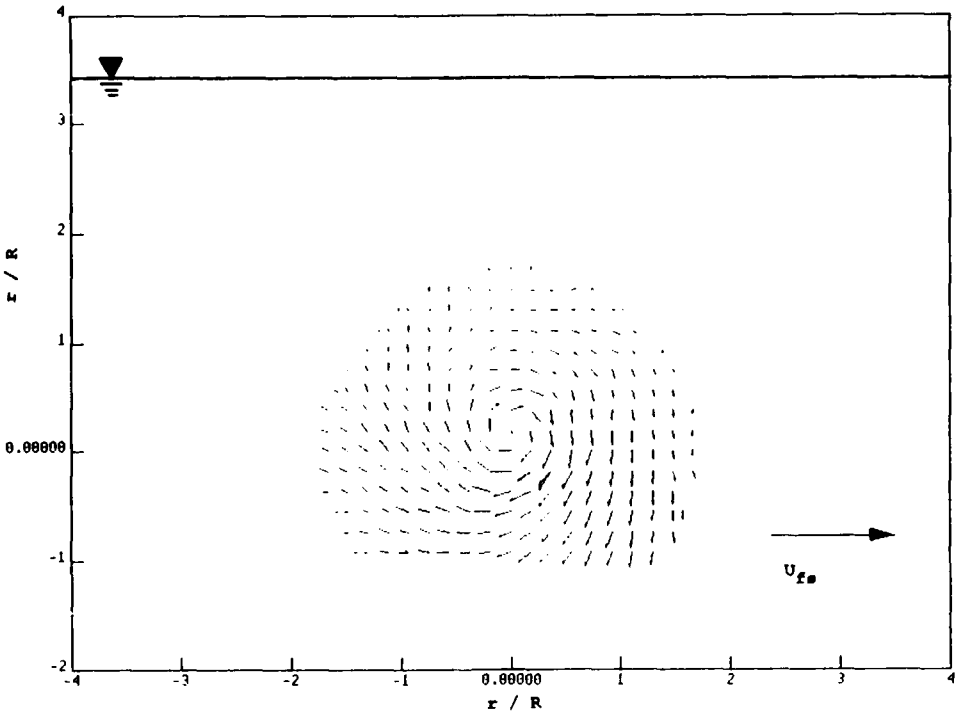

Figure 14. Plot of transverse velocity vectors in relation to the free surface, x/D = 10.0

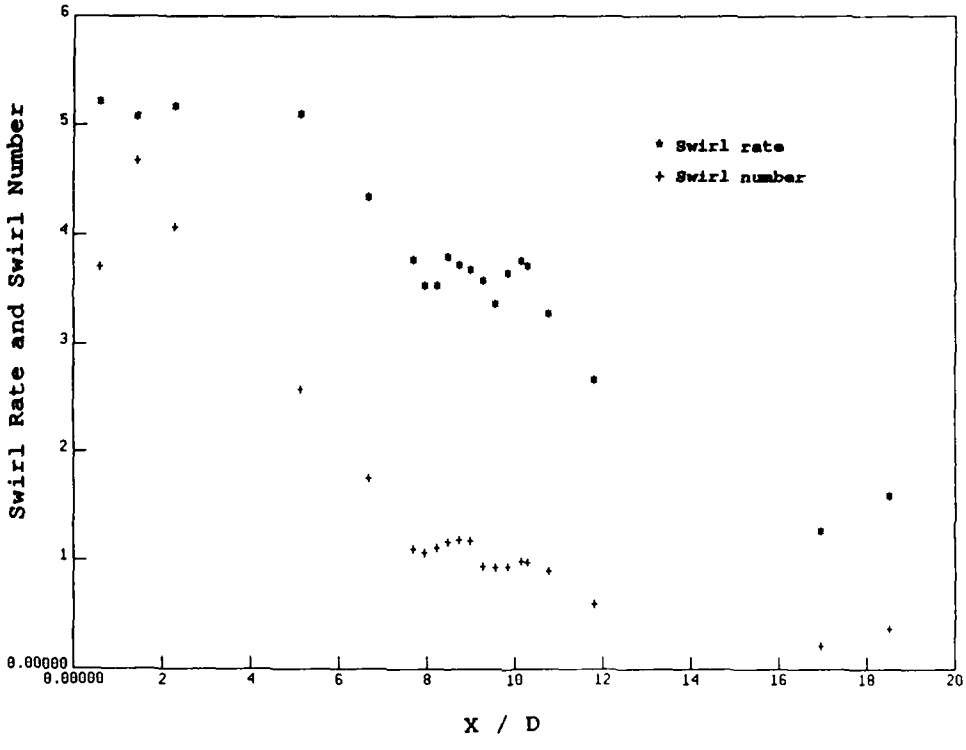

Figure 15. Plot of swirl rate and swirl number

APPENDIX A

VELOCITY MEASUREMENT CONSIDERATIONS

VELOCITY REPEATABILITY MEASUREMENTS

Repeatability measurements in the free stream determined the uncertainty for LDV velocity measurements. A standard error of the mean analysis on 6 points in the free stream resulted in an uncertainty of 0.6 percent.

Measurements were made of the repeatability of various velocity profiles. Figure A1 shows the repeatability of measuring the body of revolution wake deficit with the dummy hub installed. These profiles were taken on subsequent passes down the basin. A slight run to run bias error is observed due to carriage speed and/or prop rpm variations. The average difference in magnitude between the two profiles is approximately 3 percent.

Figures A2a and A2b show repeatability of measuring the tangential and radial velocity at a downstream position of x/D=10. These profiles were taken sequentially; however, each profile is the result of two passes down the basin. Therefore bias error is not limited to different runs. Good repeatability is seen for the tangential velocity. The radial velocity appears to be more sensitive to bias error.

Figures A3a and A3b show repeatability measurement of streamwise and radial velocity at x/D=16.5. These profiles were taken on subsequent passes. The streamwise velocity repeatability is good with an average difference in magnitude of 1.4 percent. However, the radial velocity again appears to be sensitive to bias error.

PROBE FLOW DISTURBANCE

The flow disturbance due to the probe may be estimated by calculating the potential flow disturbance at the measurement volume location for each of two

conditions corresponding to the two orientations of the probe used in this experiment (see Figure 2). Results of potential flow computation for both the probe and support strut indicated velocity bias errors of less than 0.2 percent for either probe orientation.

FLOW UNIFORMITY

A uniform inflow into the body of revolution is necessary to insure as uniform a velocity as possible into the propeller. In order to introduce enough LDV seed particles into flow to obtain a high data rate (approximately 200 points/sec), a seeding strut was necessary. This strut was positioned upstream of the model at the front of the carriage. Initially, the strut was a cylindrical tube with holes positioned along the vertical. An airfoil section with holes positioned vertically was implemented on the second test (see Figure 1b). This strut section had a maximum thickness of 1.125 inches (2.9 cm) and a chord of 2.75 inches (7.0 cm). This strut extended from the free surface to approximately 20 inches (50.8 cm) below the free surface. To vary the distance of the propeller from the measurement volume, the model was moved along the carriage girder.

Figure A4 shows transverse uniformity profiles approximately 18 feet (5.5 m) downstream of the seeding strut without a model installed. Measurements were taken at propeller center-line depth (17.8 inches (45.2 cm) below the free-surface) and 4 inches (10.2 cm) above and below the propeller center-line. A velocity defect of approximately 2 percent due to the seeding strut was measured.

BODY OF REVOLUTION WAKE MEASUREMENT

A dummy hub without blades was mounted in place of the propeller. Figure A5 shows profiles of the hull wake deficit at x/D = 0.6 with the dummy hub spinning. The influence of the strut wakes are clearly distinguishable in the z+ direction. Also shown is unpublished other DTRC wake survey bare hull data at the propeller plane. Figure A6 show profiles of the hull wake deficit at x/D = 0.6 with and without the dummy hub spinning.

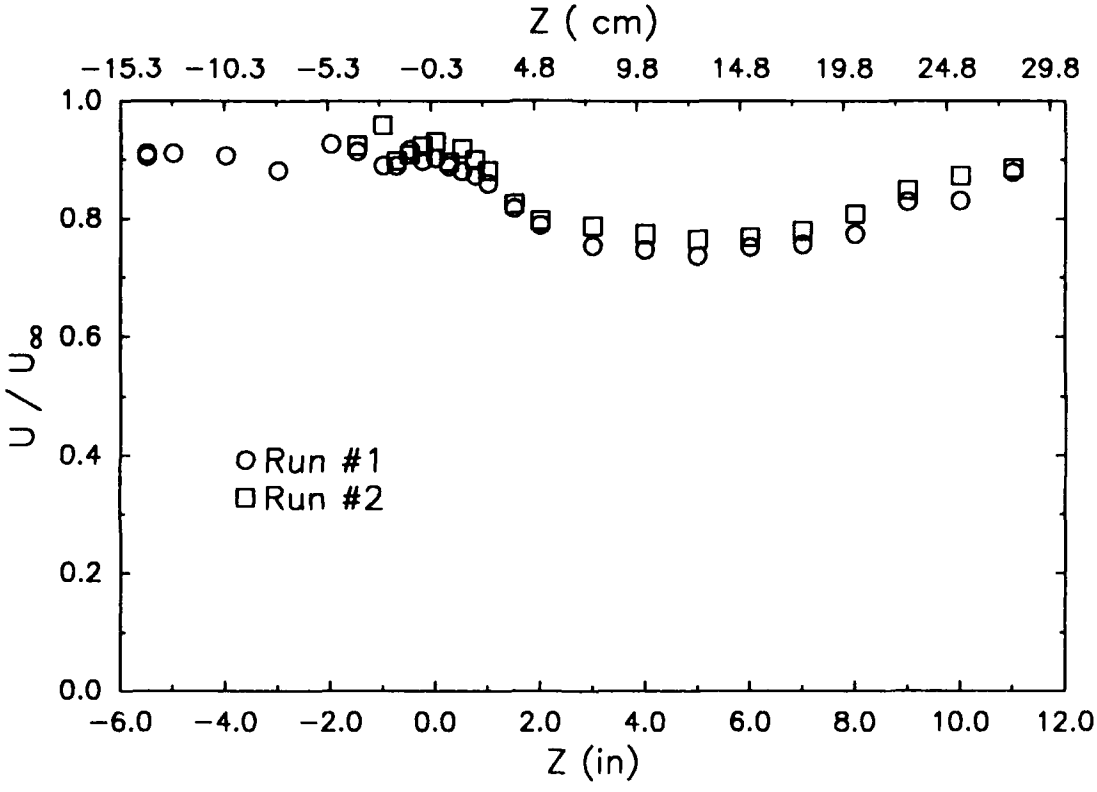

Figure A1. Wake deficit velocity repeatability (with dummy hub)

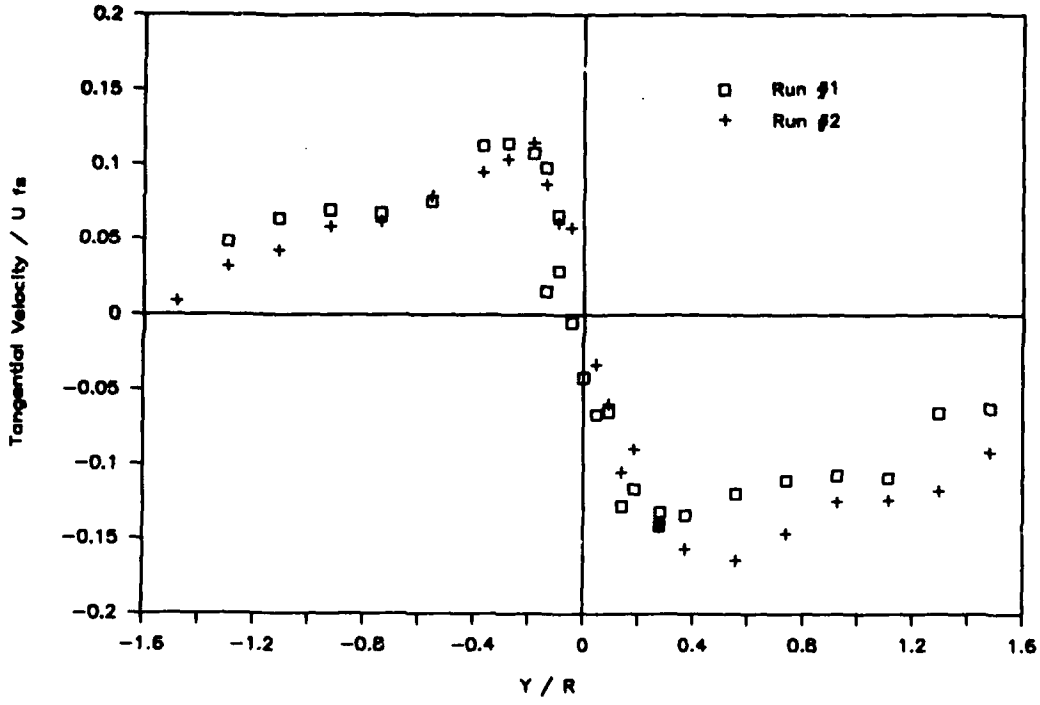

Figure A2a. Tangential velocity

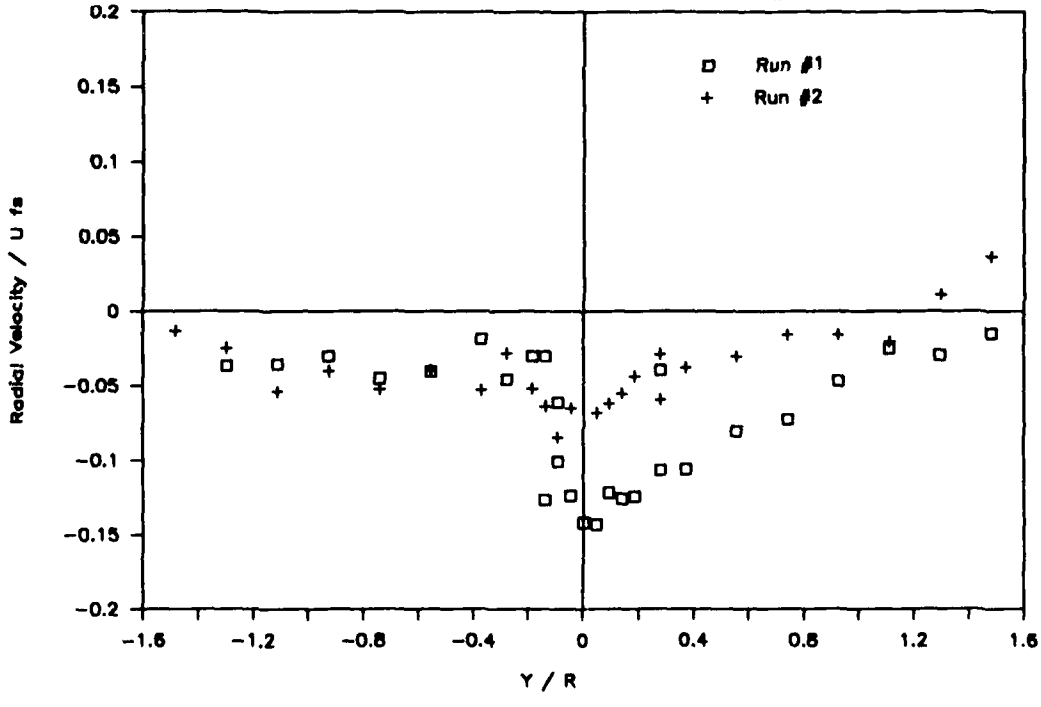

Figure A2b. Radial velocity

Figure A2. Velocity repeatability, x/D = 10.0

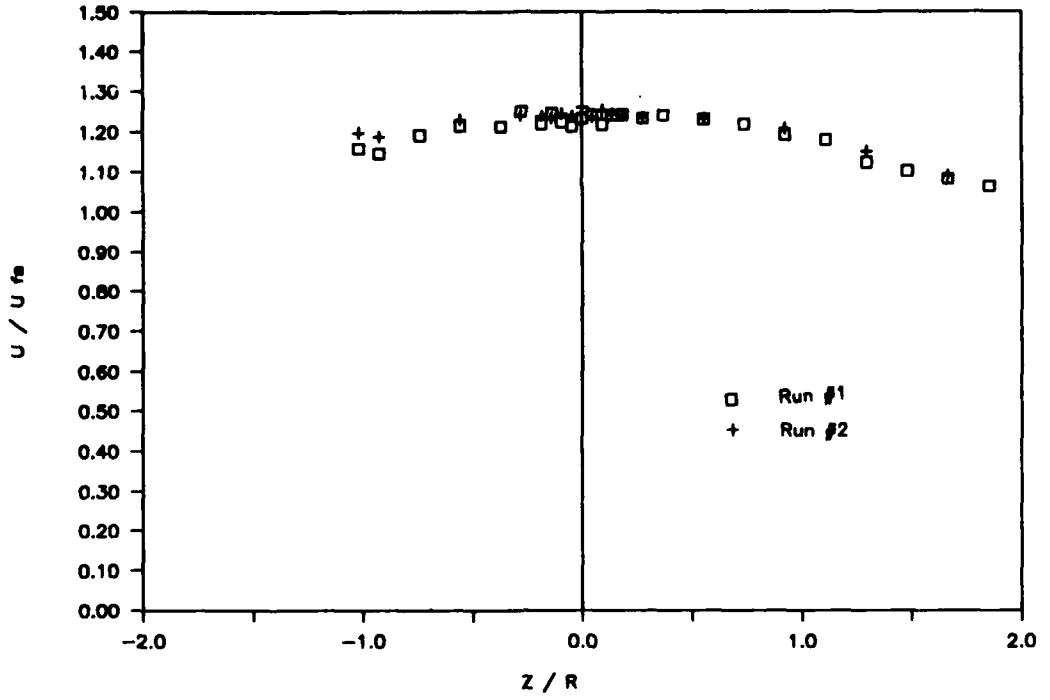

Figure A3a. Streamwise velocity

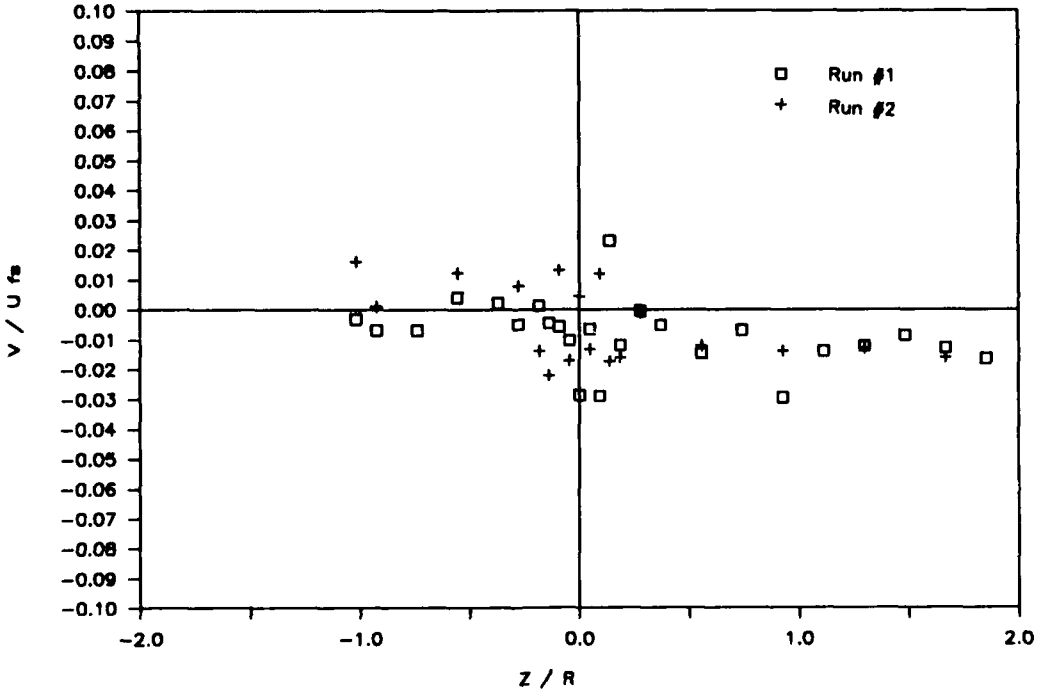

Figure A3b. Radial velocity

Figure A3. Velocity repeatability, x/D = 16.5

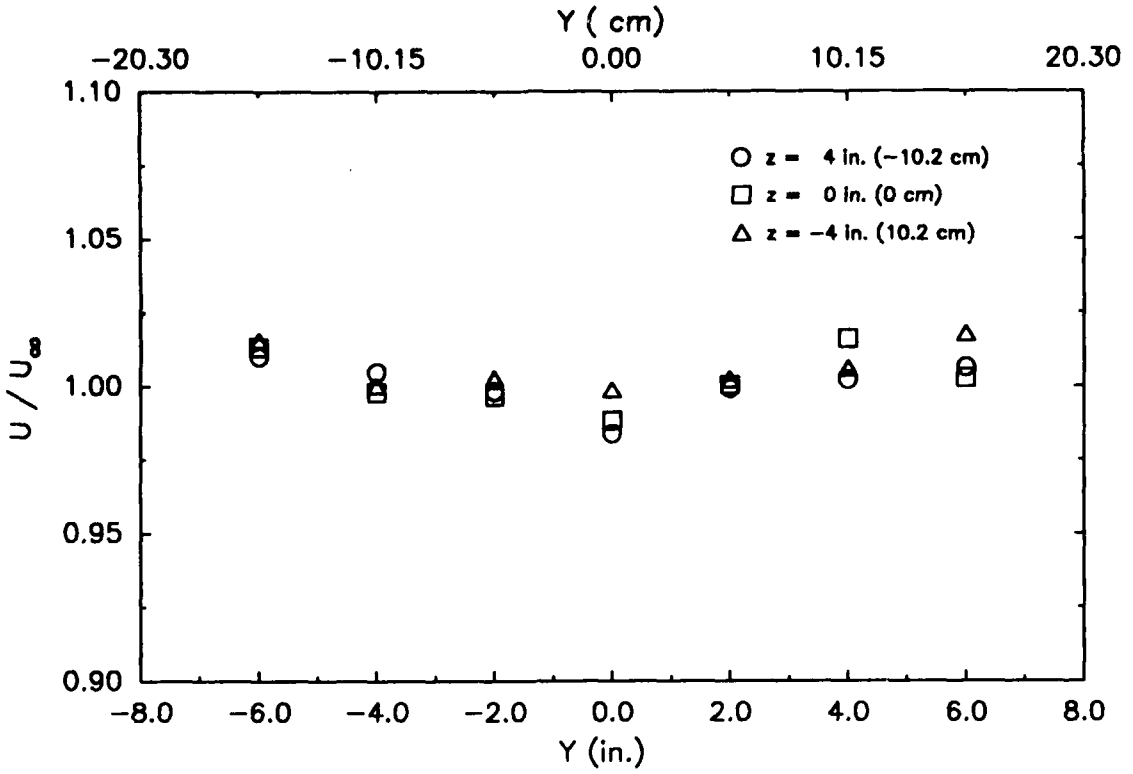

Figure A4. Streamwise velocity repeatability (without model)

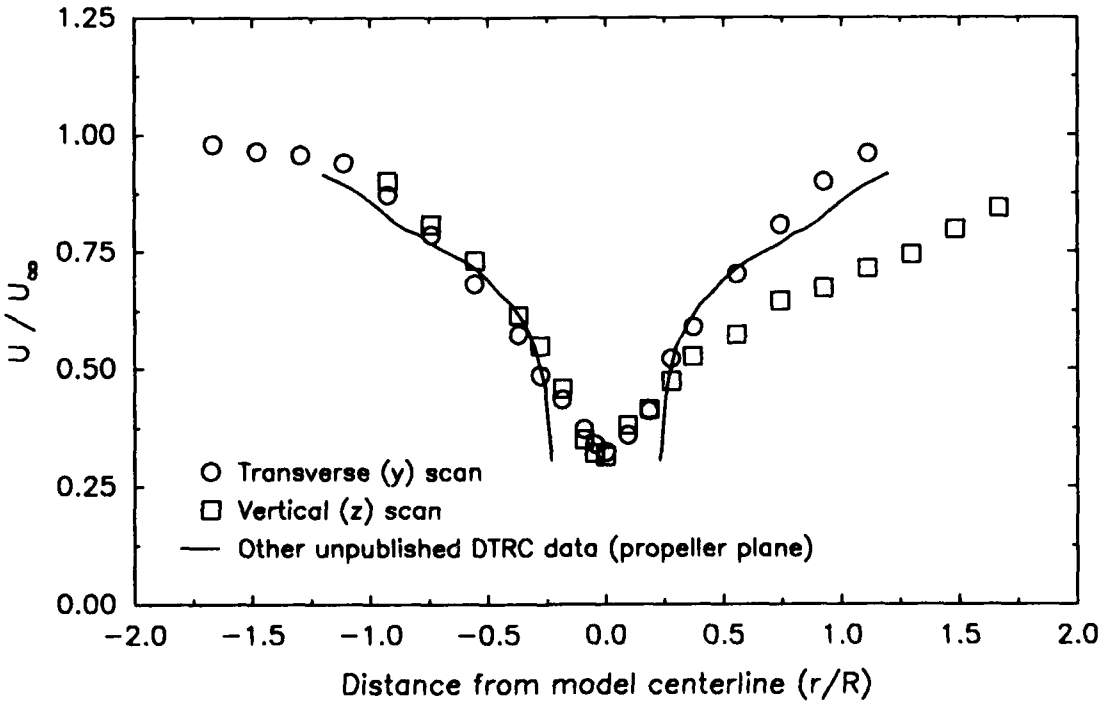

Figure A5. Mean axial velocity with spinning dummy hub, $x/D = 0.6$

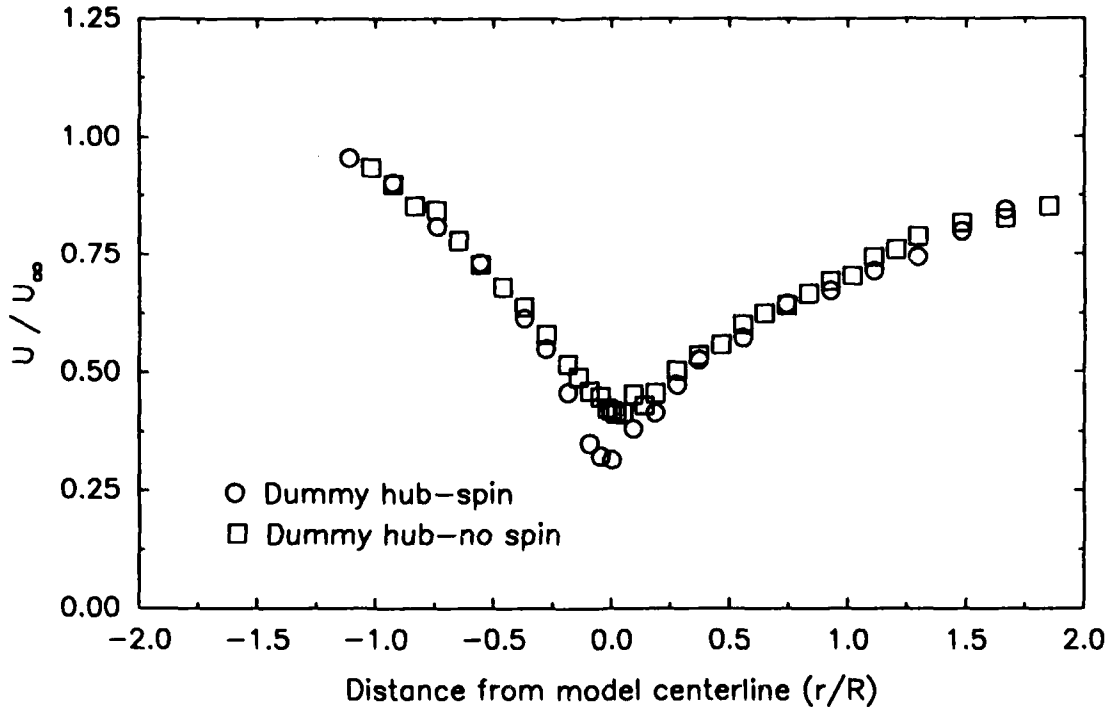

Figure A6a. Vertical scan

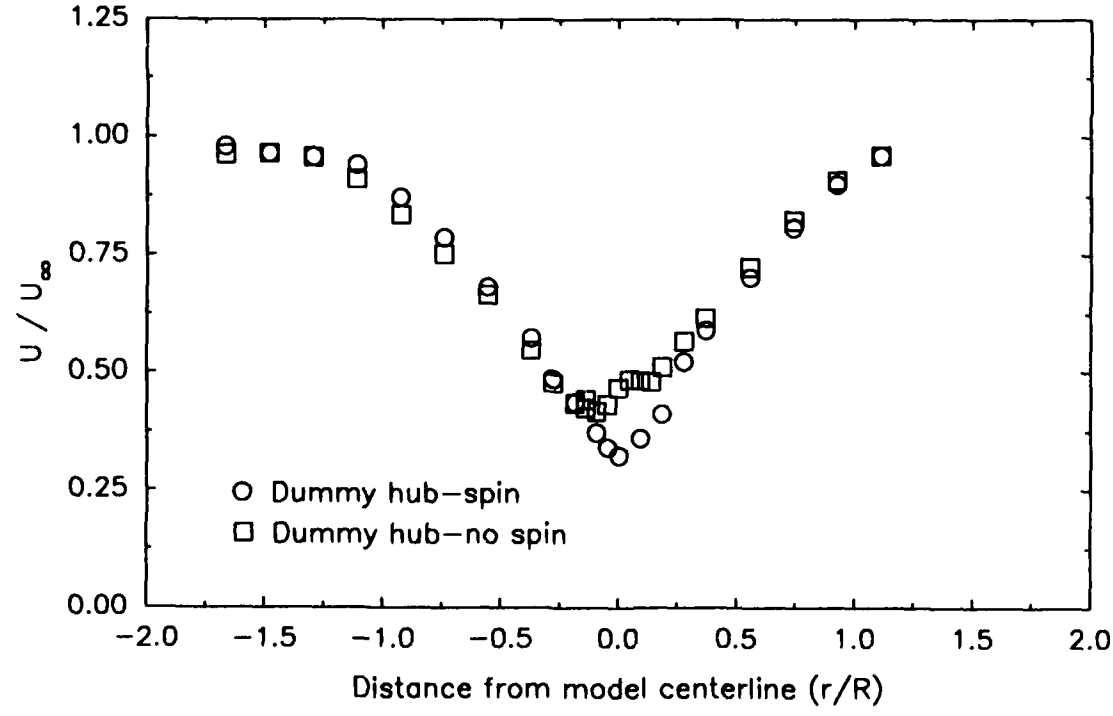

Figure A6b. Transverse scan

Figure A6. Hull wake deficit with and without spinning dummy hub, x/D = 0.6

APPENDIX B

PROPELLER CHARACTERISTICS

Characteristic open water curves for propellers #3666 and #3667 are shown in Figures B1 and B2. Propeller geometry is shown in Figures B3 and B4.

Thrust and torque measurements were performed for the operating condition of this experiment. Upon analysis, however, it was determined that these data were in error. In order to estimate the operating point, a wake fraction was estimated by integrating the velocity profiles near the propeller plane with the dummy hub installed (see Figure A5). J_T was determined using the wake fraction. C_T was then determined using J_T and the characteristic open water curves. Table B1 list these values.

Table B1. Propeller operating characteristics

	Propeller #3666	Propeller #3667
Wake fraction	0.9	0.9
J_T	0.58	0.58
C_T	1.2	1.4

REYNOLDS NUMBER, $R_e = b_{0.7}\frac{\sqrt{V_a^2+(0.7\pi nD)^2}}{\nu}$

THRUST COEFFICIENT, $K_t = \frac{T}{\rho n^2 D^4}$

TORQUE COEFFICIENT $K_q = \frac{Q}{\rho n^2 D^5}$

SPEED COEFFICIENT, $J = \frac{V_a}{nD}$

EFFICIENCY, $e = \frac{TV_a}{2\pi Qn} = \frac{K_t}{K_q} \times \frac{J}{2\pi}$

T = THRUST
Q = TORQUE
n = REVOLUTIONS PER UNIT TIME
V_a = SPEED OF ADVANCE
$b_{0.7}$ = SECTION LENGTH AT 0.7 RADIUS
D = DIAMETER
P = PITCH
ν = KINEMATIC VISCOSITY
ρ = DENSITY OF WATER

NUMBER OF BLADES	5
EXP. AREA RATIO	0.627
MWR	0.250
BTF	0.057
P/D (AT 0.7R)	0.886
DIAMETER	10.800 ins.
PITCH (AT 0.7R)	9.569 ins.
ROTATION	R.H.
TEST n	13.0 r.p.s.
TEST V_a	2.5 to 10.0 f.p.s.

23 MAY 1957
DAVID W. TAYLOR MODEL BASIN
WASHINGTON, D.C.

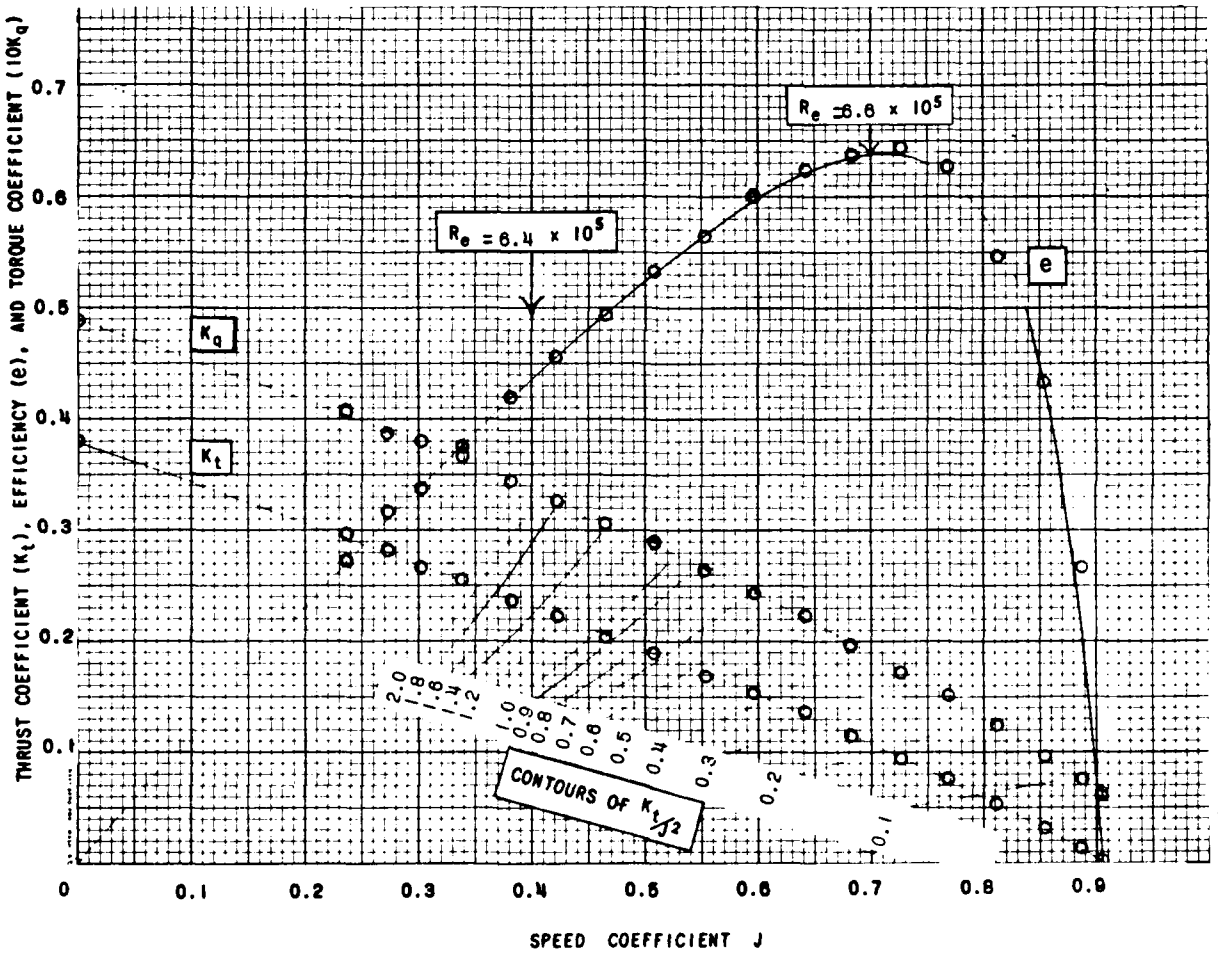

Figure B1. Characteristic curves of propeller #3666

REYNOLDS NUMBER, $R_e = b_{0.7}\frac{\sqrt{V_a^2+(0.7\pi nD)^2}}{\nu}$

THRUST COEFFICIENT, $K_t = \frac{T}{\rho n^2 D^4}$

TORQUE COEFFICIENT $K_q = \frac{Q}{\rho n^2 D^5}$

SPEED COEFFICIENT, $J = \frac{V_a}{nD}$

EFFICIENCY, $e = \frac{TV_a}{2\pi Qn} = \frac{K_t}{K_q} \times \frac{J}{2\pi}$

T = THRUST
Q = TORQUE
n = REVOLUTIONS PER UNIT TIME
V_a = SPEED OF ADVANCE
$b_{0.7}$ = SECTION LENGTH AT 0.7 RADIUS
D = DIAMETER
P = PITCH
ν = KINEMATIC VISCOSITY
ρ = DENSITY OF WATER

NUMBER OF BLADES..... 5
EXP. AREA RATIO..... 0.518
MWR..... 0.206
BTF..... 0.057
P/D (AT 0.7R)..... 0.928
DIAMETER.....10.800 ins.
PITCH (AT 0.7R).....10.020 ins
ROTATION..... R.H.
TEST n..... 12.8 r.p.s.
TEST V_a..... 2.5 to 10.0 f.p.s.

23 MAY 1957
DAVID W. TAYLOR MODEL BASIN
WASHINGTON, D.C.

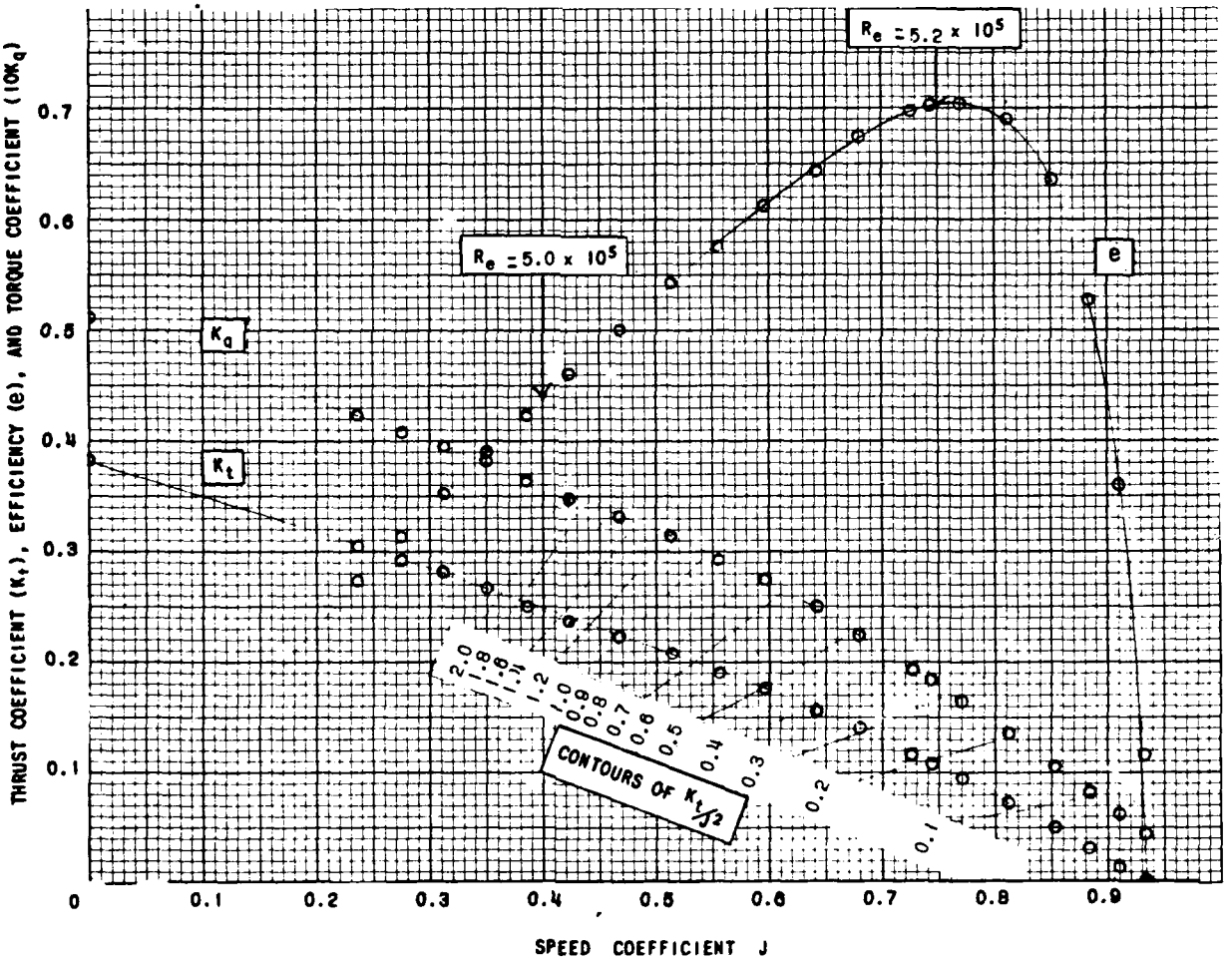

Figure B2. Characteristic curves of propeller #3667

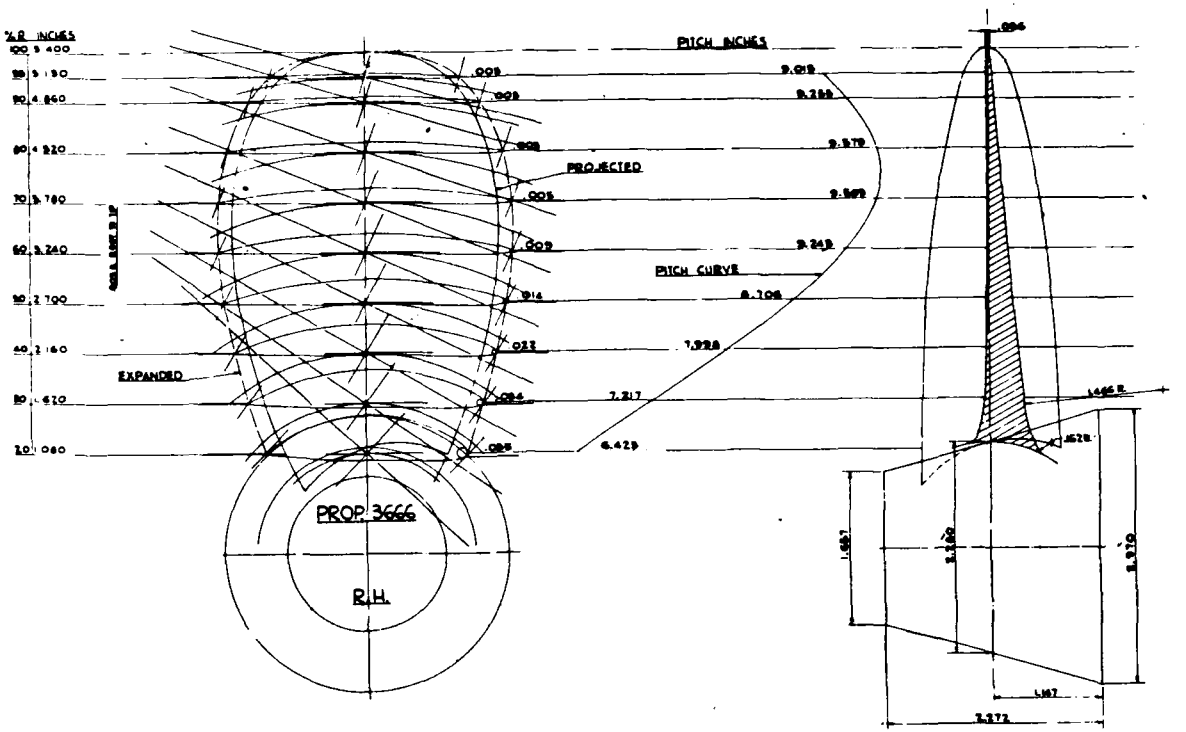

Figure B3. Propeller #3666 geometry

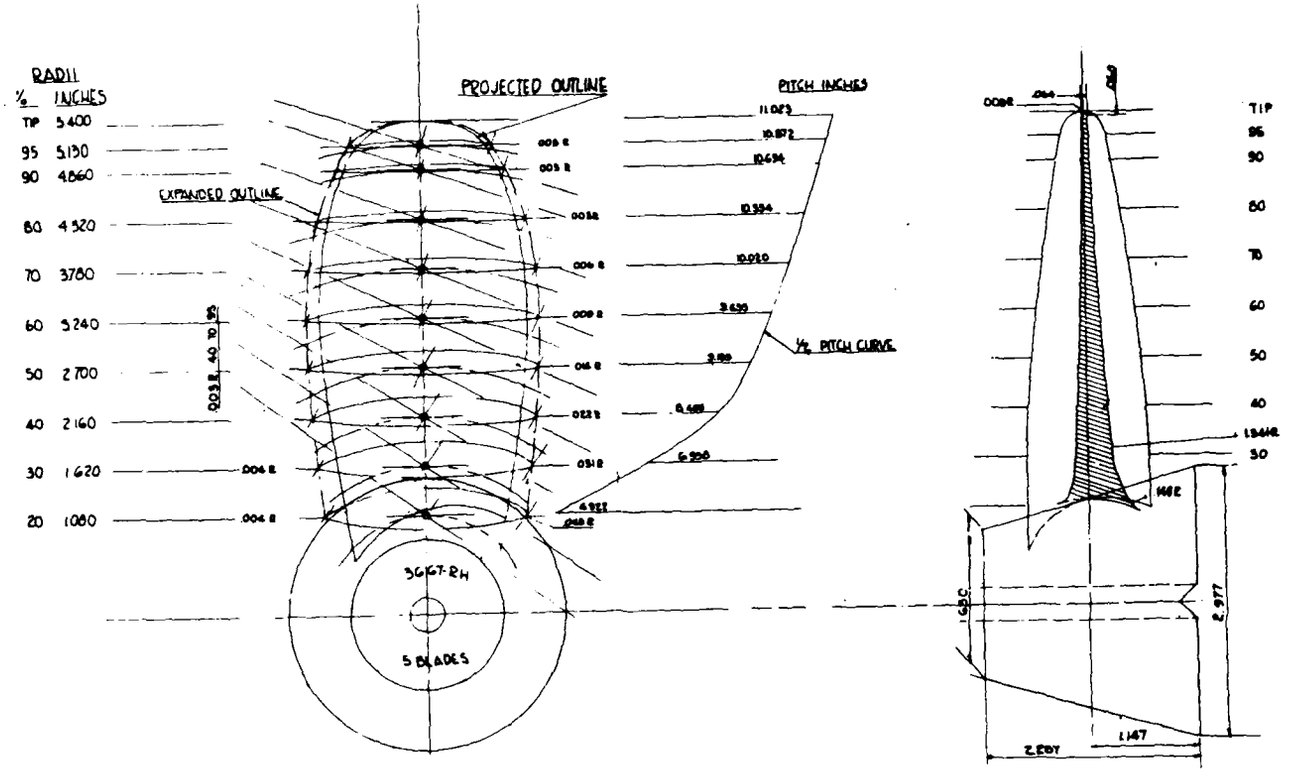

Figure B4. Propeller #3667 geometry

THIS PAGE INTENTIONALLY LEFT BLANK

REFERENCES

Blaurock, J. and G. Lammers (1986), "Measurements of the Time Dependent Velocity Field Surrounding a Model Propeller in Uniform Water Flow," AGARD–CPP–413.

Fry, D.J., S. Jessup, and T.T. Huang (1987), "Application of Laser Doppler Velocimetry for Ship Hydrodynamic Measurements," ITTC.

Jessup, S.D., C.G. Schott, M.F. Jeffers, and S. Kobayashi (1985), "Local Propeller Blade Flows in Uniform and Sheared Onset Flows Using LDV Techniques," Ship Performance Department Research and Development Report DTNSRDC–85/007.

Kotb, M.A., and J.A. Schetz (1984), "Measurements of the 3D Turbulent Flow Behind a Propeller in a Shear Flow," AIAA Paper 84–1676.

Lyden, J.D., D.R. Lyzenga, R.A. Shuchman, and E.S. Kasischke (1985), "Analysis of Narrow Ship Wakes in Georgia Strait SAR Data," Environmental Research Institute of Michigan Report 155900–20–T.

Min, K. (1978), "Numerical and Experimental Methods for the Prediction of Field Point Velocities Around Propeller Blades," MIT Report 78–12.

Nagle, T.J., and J.F. McMahon (1985), "Flow Velocity Measurements in the Vicinity of a Set of Contrarotating Research Propellers (Propellers 4866 and 4867) Using Laser Doppler Velocimetry," Ship Performance Department Report DTNSRDC/SPD–596–04.

Swean, T.F. (1987), "Numerical Simulation of the Wake Downstream of a Twin–Screw Destroyer Model," NRL Memorandum Report 6131.

Wang, M. (1985), "Hub Effects in Propeller Design and Analysis," MIT Report 85–14.

DTNSRDC ISSUES THREE TYPES OF REPORTS:

1. **DTNSRDC reports, a formal series,** contain information of permanent technical value. They carry a consecutive numerical identification regardless of their classification or the originating department.

2. **Departmental reports, a semiformal series,** contain information of a preliminary, temporary, or proprietary nature or of limited interest or significance. They carry a departmental alphanumerical identification.

3. ***Technical memoranda, an informal series,*** contain technical documentation of limited use and interest. They are primarily working papers intended for internal use. They carry an identifying number which indicates their type and the numerical code of the originating department. Any distribution outside DTNSRDC must be approved by the head of the originating department on a case-by-case basis.